NASA/CR—2000-210072

Evaluation of Trapped Radiation Model Uncertainties for Spacecraft Design

T.W. Armstrong and B.L. Colborn
Science Applications International Corporation, Prospect, TN

Prepared for Marshall Space Flight Center
under Contract NAS8-40294
and sponsored by
The Space Environments and Effects Program
managed at the Marshall Space Flight Center

March 2000

The NASA STI Program Office...in Profile

Since its founding, NASA has been dedicated to the advancement of aeronautics and space science. The NASA Scientific and Technical Information (STI) Program Office plays a key part in helping NASA maintain this important role.

The NASA STI Program Office is operated by Langley Research Center, the lead center for NASA's scientific and technical information. The NASA STI Program Office provides access to the NASA STI Database, the largest collection of aeronautical and space science STI in the world. The Program Office is also NASA's institutional mechanism for disseminating the results of its research and development activities. These results are published by NASA in the NASA STI Report Series, which includes the following report types:

- TECHNICAL PUBLICATION. Reports of completed research or a major significant phase of research that present the results of NASA programs and include extensive data or theoretical analysis. Includes compilations of significant scientific and technical data and information deemed to be of continuing reference value. NASA's counterpart of peer-reviewed formal professional papers but has less stringent limitations on manuscript length and extent of graphic presentations.

- TECHNICAL MEMORANDUM. Scientific and technical findings that are preliminary or of specialized interest, e.g., quick release reports, working papers, and bibliographies that contain minimal annotation. Does not contain extensive analysis.

- CONTRACTOR REPORT. Scientific and technical findings by NASA-sponsored contractors and grantees.

- CONFERENCE PUBLICATION. Collected papers from scientific and technical conferences, symposia, seminars, or other meetings sponsored or cosponsored by NASA.

- SPECIAL PUBLICATION. Scientific, technical, or historical information from NASA programs, projects, and mission, often concerned with subjects having substantial public interest.

- TECHNICAL TRANSLATION. English-language translations of foreign scientific and technical material pertinent to NASA's mission.

Specialized services that complement the STI Program Office's diverse offerings include creating custom thesauri, building customized databases, organizing and publishing research results...even providing videos.

For more information about the NASA STI Program Office, see the following:

- Access the NASA STI Program Home Page at ***http://www.sti.nasa.gov***

- E-mail your question via the Internet to help@sti.nasa.gov

- Fax your question to the NASA Access Help Desk at (301) 621–0134

- Telephone the NASA Access Help Desk at (301) 621–0390

- Write to:
  NASA Access Help Desk
  NASA Center for AeroSpace Information
  7121 Standard Drive
  Hanover, MD 21076–1320

NASA/CR—2000-210072

Evaluation of Trapped Radiation Model Uncertainties for Spacecraft Design

T.W. Armstrong and B.L. Colborn
Science Applications International Corporation, Prospect, TN

Prepared for Marshall Space Flight Center
under Contract NAS8-40294
and sponsored by
The Space Environments and Effects Program
managed at the Marshall Space Flight Center

National Aeronautics and
Space Administration

Marshall Space Flight Center • MSFC, Alabama 35812

March 2000

Available from:

NASA Center for AeroSpace Information
7121 Standard Drive
Hanover, MD 21076–1320
(301) 621–0390

National Technical Information Service
5285 Port Royal Road
Springfield, VA 22161
(703) 487–4650

Table of Contents

Evaluation of Trapped Radiation Model Uncertainties for Spacecraft Design

1. Introduction and Summary

1.1 Background

Trapped radiation models which describe the characteristics of protons and electrons in the Van Allen belts are essential in addressing numerous Earth-orbit spacecraft and mission design issues related to the ionizing radiation environment, such as parts selection and placement, component lifetimes, performance degradation, and orbit parameters to minimize risk. The de-facto standard models used internationally for predicting trapped radiation environments (AP8 for protons and AE8 for electrons, developed by Vette and colleagues [1-3]) are based on old and incomplete flight data collected 2-3 decades ago.

While new models are needed, it is expected to be some time before sufficient flight data are available to allow new models to be generated with the general capabilities in terms of complete inclination and altitude coverage as currently provided by AP8 and AE8. In the meantime, designers are confronted with specifying spacecraft and mission requirements and radiation designs using AP8 and AE8, which do not reflect what has been learned from trapped radiation flight measurements during the past decade or longer.

1.2 Study Objectives

The objectives of the present work are: (a) to evaluate AP8 and AE8 model uncertainties based on comparisons with various sets of recent satellite data, and (b) to derive "empirical correction factors" which designers can apply to AP8 and AE8 results so that the models will be more consistent with recent flight data. Thus, the aim is to distill from various flight observations and publications simple model correction factors that have adequate accuracy for engineering-type applications and can be readily applied by the spacecraft designer.

1.3 Study Products

In this report a summary of AP8 and AE8 model comparisons with flight data is given, mainly in terms of measured-to-predicted ratios for various orbit inclinations and altitudes. Values for the model predictions and flight data and additional details of the model-data comparisons are given in a companion report [4]. Also included in the companion report are model-model comparisons for the standard AP8 and AE8 models, the European Space Agency versions of AP8 and AE8, and Russian trapped radiation models. In addition, as part of the present study ionizing radiation environments and effects from Russian satellite measurements were assimilated and assessments made on the suitability of these data sets for AP8 and AE8 model validation applications [5].

Another product from this study is the TRAP/SEE code, a PC version of the standard and European Space Agency versions of the AP8 and AE8 models with a convenient user interface, an accurate orbit code for treating highly elliptical as well as circular orbits, and user documentation [6]. (The code is available from the Space Environments and Effects Program Office, NASA Marshall Space Flight Center, http://see.msfc.nasa.gov/.) Factors which can influence the predictions made using different implementations of the AP8 and AE8 models are discussed in [6].

1.4 Summary Conclusions for Design Applications

While current flight data available for model comparisons are not sufficiently complete to quantify model uncertainties for all orbit environments, radiation effects, and extreme geomagnetic activity conditions of interest, there are two cases, described below, where sufficient data are available to provide definitive model uncertainty estimates. Model correction factors for these two cases are considered sufficiently accurate that they can be applied in spacecraft design applications and in setting radiation design margins.

1.4.1 AP8 Model for Low Altitude Orbits

From comparisons of the AP8 trapped proton model with several sets and types of flight data (flux, dose, and activation) at low altitudes (below about 2000 km, where most of the flight data are available for comparison), it is found that the AP8 model underpredicts by about a factor of 2. By multiplying the AP8 model output fluxes by a

factor of 2, the resulting corrected model predictions are within about ± 25% of the flight data, as discussed in Sec. 3.1.1. This empirical factor of 2 correction applies to both AP8MIN and AP8MAX predictions and is independent of proton energy (at least for energies above about 15 MeV, the energy range where model checks against flight data have been made).

This factor of 2 correction applies, of course, only for situations where the AP8 model is used within the inherent limitations of the model; these limitations are summarized in Sec. 3.5.3. In particular, this correction factor is not generally applicable for short duration flights such as the Space Shuttle, as shown in Sec. 3.5.2.

1.4.2 AE8 Model at High Altitudes

The AE8 trapped electron model clearly overpredicts the electron fluxes in the outer electron belt. During periods of normal geomagnetic activity, the overprediction is a factor of 5 to10 in the peak regions of the outer belt and a factor of 10 to 100 in the outer regions of the belt (which includes geosynchronous satellite altitudes). The AE8 model overprediction is so large that electron fluxes in the outer belt are still overstimated even for highly enhanced transient flux conditions caused by large geomagnetic disturbances (Sec. 4.1.3).

1.4.3 Other Cases

For other cases (AP8 at high altitudes, AE8 at low altitudes, quiet vs. active geomagnetic conditions), some flight data are available that provide insight on model uncertainties, but the data–model comparisons are not considered sufficiently complete to extract definitive model uncertainty factors. These comparisons are discussed in Secs. 3.1.2 and 3.6.2 for protons at high altitudes, in Secs. 4.1.1 and 4.2 for electrons at low altitudes, and the influence of high geomagnetic activity is discussed in Secs. 3.6.2, 4.1.1, 4.1.3, and 4.2.

1.4.4 Implications for Spacecraft Design

A common procedure used in designing spacecraft to withstand the trapped proton environment has been to use the AP8 model for environment predictions and then apply a

design margin (commonly a factor of 2) to the AP8 output spectra for use in predicting radiation effects. The results here show that the AP8 flux predictions are a factor of 2 too low. Thus, using the common procedure the design margin is consumed by the AP8 model error. The results here suggest that a factor of 2 correction to the AP8 results should be applied and then a design margin applied.

The large AE8 model overpredictions can have important consequences related to spacecraft design. For example, if designers use the standard AE8 output, and then apply conservative safety factors to the environment predictions, which is a common procedure, then the radiation requirements most likely will be significantly overestimated for most radiation effects – e.g., the use of radiation hardened parts may be indicated but not actually needed.

2. Approach

2.1 Flight Data

Summarized below are features and application limitations of the data sets which have been used in evaluating AP8 and AE8 model uncertainties.

2.1.1 CRRES

The Combined Release and Radiation Effects Satellite (CRRES) made several types of radiation measurements in a geosynchronous transfer orbit (18.2° inclination, 327 km perigee, 33,575 km apogee) over a 14 month period (July 1990 to October 1991) during the maximum of Solar Cycle 22 [7, 8]. A unique feature of the CRRES data is that during the mission (23-31 March 1991) an extraordinarily large geomagnetic storm occurred in conjunction with an intense solar proton event, resulting in a strong shock front hitting the magnetosphere and greatly enhanced radiation belt fluxes, which gradually decayed over a year or so. Thus, CRRES data are available for a "quiet" magnetic activity period of 8 months prior to the storm and an "active" period of high magnetic activity and enhanced flux levels for 6 months after the storm. We have used the following four data sets from the CRRES mission for model comparisons.

Space Radiation Dosimeters

These detectors measured the dose in silicon semiconductors under aluminum hemispheres having four different thicknesses (0.57, 1.59, 3.14, and 6.08 g/cm^2), corresponding to energy thresholds of 1, 2.5, 5, and 10 MeV for electrons and 20, 35, 50, and 75 MeV for protons [9]. Dose contributions were obtained separately for low LET particles (protons > 100 MeV, electrons, and bremsstrahlung) and high LET particles (20 – 100 MeV protons and > 5 MeV electrons).

The CRRES dose values compared with here were generated using the CRRESRAD software package [10] from Phillips Laboratory (Hanscom AFB) in which the flight data have been organized in B/B_o and L coordinates so that orbit-average doses for different orbit parameters can be determined. Although the CRRES orbit perigee was 350 km, statistics at the lowest altitudes are poor, and the data are applicable only for

altitudes above about 800 km. The data are most accurate for inclinations below about 30° (magnetic), but CRRESRAD can be applied for higher inclination orbits for the thicker shielding (3.14 and 6.08 g/cm^2) where the dose is dominated by protons [10].

PROTEL Detector

A proton telescope (PROTEL) detector on CRRES measured protons in the 1-100 MeV range in 24 energy steps [11]. Corrections to the data were made to remove contamination by out-of-aperture protons slowing down and being counted. These corrections become increasingly less reliable for altitudes below 2500 km [11], so we have used PROTEL data only down to 1500 km. As with the CRRES dose rate, a PROTEL data base in B/B_0 – L space has been generated by Phillips Laboratory and incorporated in a software package called CRRESPRO [12] for determining proton flux for other orbits. The CRRESPRO code, which is applicable for all inclinations, was used here for the comparisons with CRRES proton measurements.

HEEF Detector

The High Energy Electron Fluxmeter (HEEF) detector on CRRES measured electrons in 10 energy intervals from 0.5 to 6.60 MeV. The software utility CRRESELE [13] was used here to access the measurement data base and compute orbit average fluxes at different altitudes. These electron measurements are limited to the outer zone electron belt in the region from about L = 2.5 to 6.80. To provide information on flux enhancement dependence on magnetic activity level, the fluxes in the CRRESELE data bases are separated into bins according to Ap_{15}, a 15-day running average of the 3-hour Ap magnetic activity index.

MEA Detector

The Medium Electron A (MEA) electron spectrometer on CRRES measured outer zone electrons in the energy range from 90 keV to 1.7 MeV. Vampola [14] has extended the energy range up to 7 MeV and down to 40 keV using OV1-19 satellite data and incorporated this CRRES mission average data into a model called ESA-SEE1. This model was then included in an updated version of the RADMODLS code [15] so that

orbit-average electron spectra in the outer zone can be calculated using the ESA-SEE1 model based on MEA data with OV1-19 energy extrapolation instead of AE8. We have used RADMODLS with the ESA-SEE1 data base to compare outer zone electron fluxes with AE8 predictions and with CRRESELE calculations based on the CRRES HEEF instrument.

2.1.2 APEX

The Advanced Photovoltaic and Electronics Experiments (APEX) satellite was operational from August 94 to June 96 (near solar minimum) in an elliptical 362 km x 2544 km orbit at 70° inclination [16]. APEX carried radiation detectors for silicon dose measurements of the same design as described above for CRRES except that on APEX the detector with thinnest shielding was a slab of aluminum 4.29 mils (0.0294 g/cm^2) thick. The other three detectors on APEX had hemispherical aluminum shields like on CRRES with thicknesses of 0.57, 1.59, and 3.14 g/cm^2. The energy thresholds for particles penetrating the shielding and being detected are, in order of increasing shielding thickness, 0.15, 1.0, 2.5, and 5.0 MeV for electrons, and 5, 20, 35, and 52 MeV for protons. At higher inclinations and thin (< 1 g/cm^2) shielding, dose from the "horns" of the outer zone electrons, which can have high variability depending on magnetic activity, make a significant contribution to the dose. Thus, the APEX dose data have been binned in intervals according to the magnetic activity index Ap_{15}. We have determined dose values in the altitude range 300 – 2000 km and at various inclinations from APEX measurements by using the APEXRAD software utility [17].

2.1.3 DMSP

The Defense Meteorological Support Program (DMSP) F7 satellite (840 km, 98.8° inclination) also carried a version of the Space Radiation Dosimeter as on CRRES and APEX for measuring silicon dose. The hemispherical aluminum shielding thicknesses for the four detectors (0.55, 1.55, 3.05, and 5.91 g/cm^2) are only slightly different than used on CRRES. Measurements have been made during the 1984 – 1987 solar minimum. Here we have used DSMP dose values quoted in the literature [18].

2.1.4 NOAA

The National Oceanic and Atmospheric Administration (NOAA) has flown radiation detectors of essentially the same design on its weather satellites (850 km, 99°) since 1978. One of the radiation sensors, the Medium Energy Proton and Electron Detector (MEPED), consists of planar silicon detectors behind hemispherical shields of different thicknesses to provide integral proton fluxes > 16, > 36, and > 80 MeV.

Huston and Pfitzer [19, 20] have recently analyzed the MEPED data from seven NOAA satellites covering the period from 1978 through 1995 (1.5 solar cycles). This data base has been incorporated into a model, NOAAPRO, with associated FORTRAN routines so that orbit-average integral fluxes for the above thresholds can be calculated (below 850 km) for an input ephemeris file. We have made calculations using NOAAPRO, with the ephermis file generated using the MSFC Burrell orbit code [21], to compare with AP8MIN and AP8MAX model predictions.

2.1.5 LDEF

The Long Duration Exposure Facility (LDEF) satellite was on-orbit for almost six years and carried some 15 experiments for measuring the ionizing radiation environment and effects [22]. The LDEF orbit was at 28.5° inclination, 479 km altitude at insertion, and 319 km at the time of Shuttle recovery; the nominal average altitude for radiation exposure was about 450 km.

Calculations have been previously made to compare AP8 model predictions with LDEF radiation measurements, with emphasis on comparing with dose measurements by thermoluminescent dosimeters (TLDs) and the induced radioactivity (activation) measurements made for various material samples and spacecraft components [23, 24]. Detailed calculations were made, taking into account the anisotropy of the trapped proton environment and shielding distributions based on a detailed 3-D mass model of the spacecraft and experiments, so that differences between measurements and predictions could be attributed to inaccuracies in the ambient environment predicted using the AP8 model. The major results from these LDEF model-data comparisons, from [23] and [24], are used here.

2.1.6 Shuttle

Extensive LEO radiation dose data are available from measurements made on the Space Shuttle, and we have made predictions to compare with the dose measurements for 63 Shuttle flights at low- (28.5°) and mid- (51.6°, 57°) inclinations in the altitude range from about 300 – 600 km [4]. These comparisons are discussed in Sec. 3.5.

2.2 Models

Flight data are compared here with predictions made using the Vette, et al. [1-3] trapped proton models for solar minimum and maximum, AP8MIN and AP8MAX, and trapped electron models at solar minimum and maximum, AE8MIN and AE8MAX, as implemented in software packages at NASA MSFC. The magnetic field models used are the 80-term International Geomagnetic Reference Field for 1965.0 [25] projected to 1964 for solar minimum calculations and the U.S. Coast and Geodetic Survey 168-term geomagnetic field model for 1970 [26] for solar maximum calculations. The magnetic moment is calculated from the field model expansion coefficients for the epoch of the field. The B and L calculations are made using the ALLMAG code and associated subroutines [27]. These models are coupled with the MSFC orbit code written by Burrell [21] to obtain orbit-average flux spectra. Dose calculations have been made using the Shieldose-2 code [28]. In comparing with hemispherical shield detectors, we have used one-half the calculated dose at the center of a spherical aluminum shield with 4π steradian incident flux.

3. Trapped Proton Model Uncertainties

3.1 Model-Data Comparisons

3.1.1 Low Altitudes

Figures 1-3 show the ratio of flight measurements to predictions using AP8MIN or AP8MAX for low (< 2000 km) altitudes and 28.5°, 51.6°, and 90° inclination orbits, respectively. The horizontal lines on these graphs are included to show that for these altitudes the measured/AP8 ratios are all within approximately 25% of a factor of two.

3.1.2 High Altitudes

For higher altitudes, Fig. 4 shows a comparison of AP8MAX with CRRES measurements (PROTEL detector) for protons > 30 MeV vs. altitude. The CRRES data are shown as an average over the 8 months prior to the very large geomagnetic storm which occurred during the mission ("Quiet" curve) and as an average over the 6-month period immediately after the storm ("Active" curve). The peak during the active period of high magnetic activity near 8,000 km indicates the formation of a temporary second proton belt. (Measurements [29] indicate that the e-folding time for the decay of the second proton belt was ten months, and proton intensities in the second belt returned to quiescent values within eighteen months.) These results show that the underprediction by AP8MAX at low altitudes continues to about 5,000 km, just past the peak of the belt. At higher altitudes, the model overpredicts during quiet times and underpredicts during the active period.

Figure 5 also shows a model-data comparison at high altitudes but using the CRRES dose data for 3.14 g/cm^2 shielding. For this shielding thickness and low activity, the dose is dominated by protons except at altitudes beyond about 10,000 km where the bremsstrahlung from outer zone electrons makes a significant contribution, producing a local maximum at 20,000 km. For the inner belt and low activity, these dose comparisons are consistent with the flux comparisons of Fig. 4; i.e., AP8MAX underestimates up to about 5,000 km and then overestimates in the outer region of the proton belt from about 5,000–10,000 km. Since the static AP8MAX model does not take into account variations due to geomagnetic activity, Figs. 4 and 5 show that the AP8 model can grossly

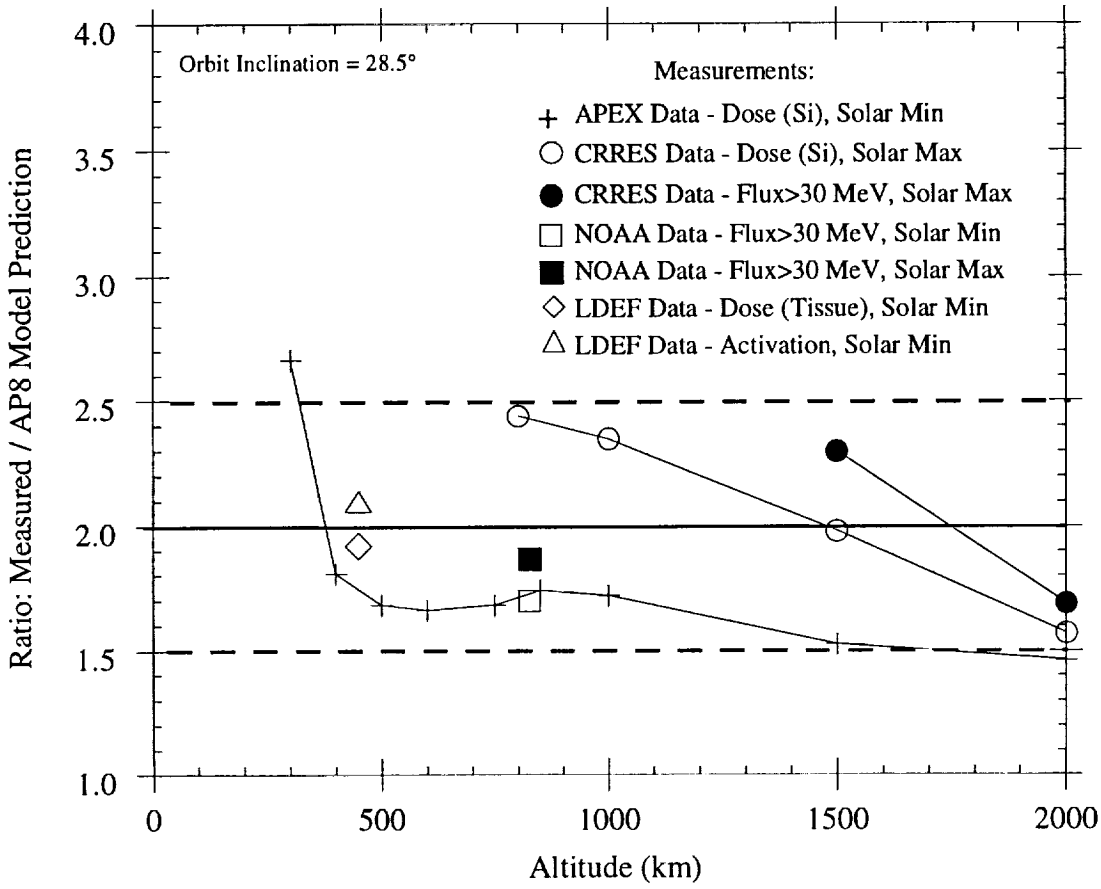

Fig. 1. Comparison of flight data with predictions using AP8 trapped proton model – for circular orbits with 28.5 ° inclination.

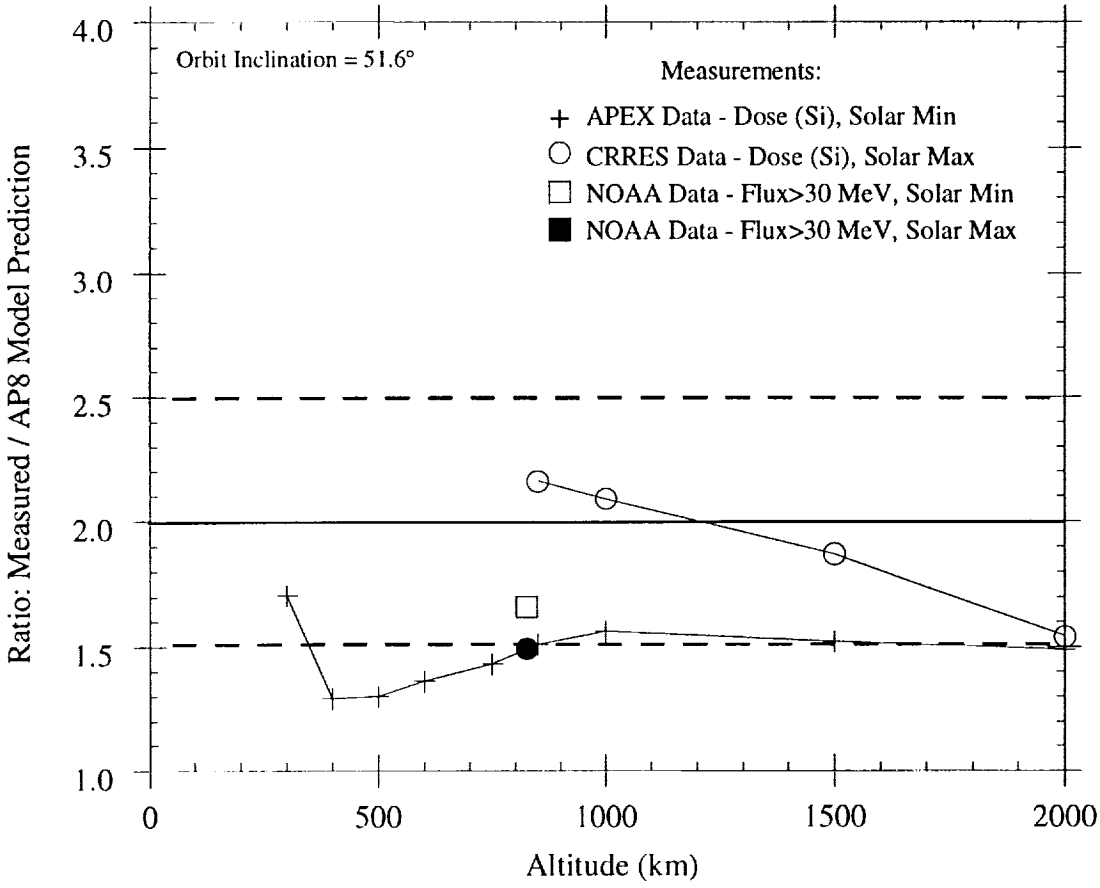

Fig. 2. Comparison of flight data with predictions using AP8 trapped proton model – for circular orbits with 51.6 ° inclination.

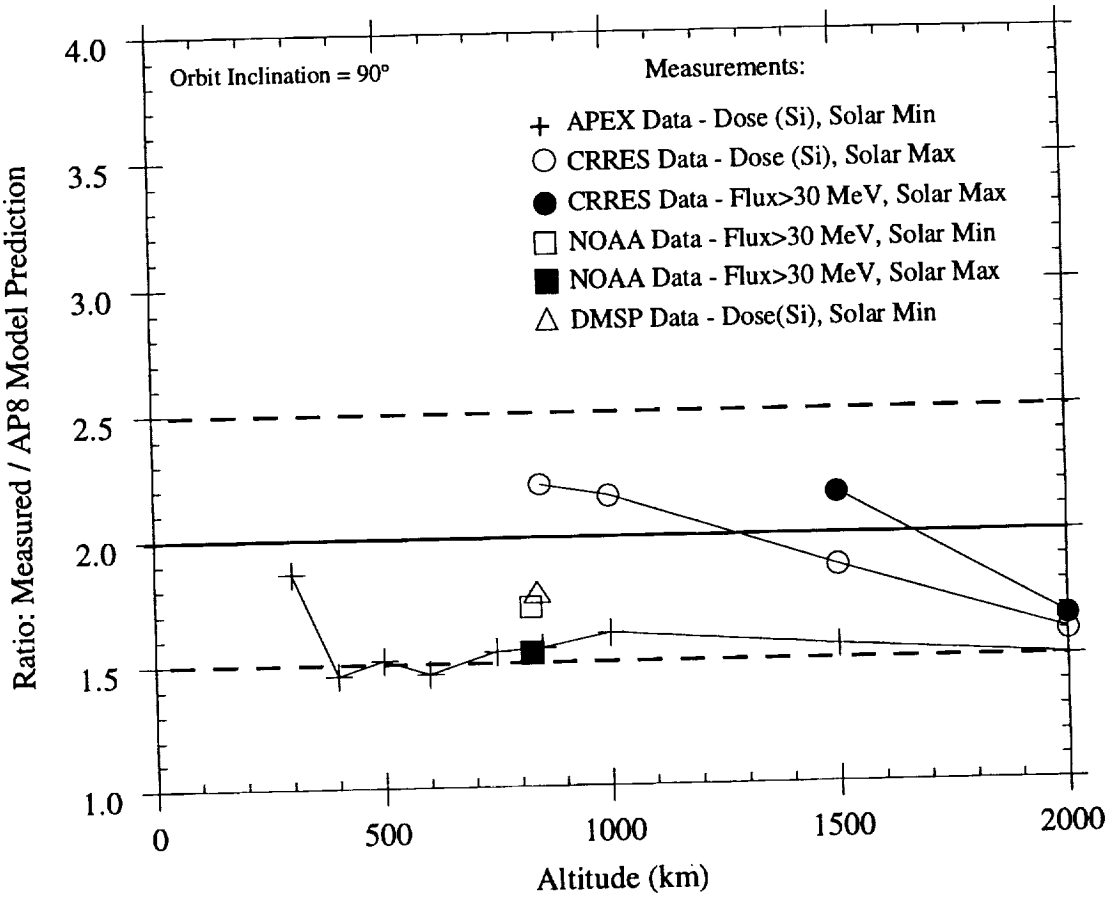

Fig. 3. Comparison of flight data with predictions using AP8 trapped proton model – for circular orbits with 90° inclination.

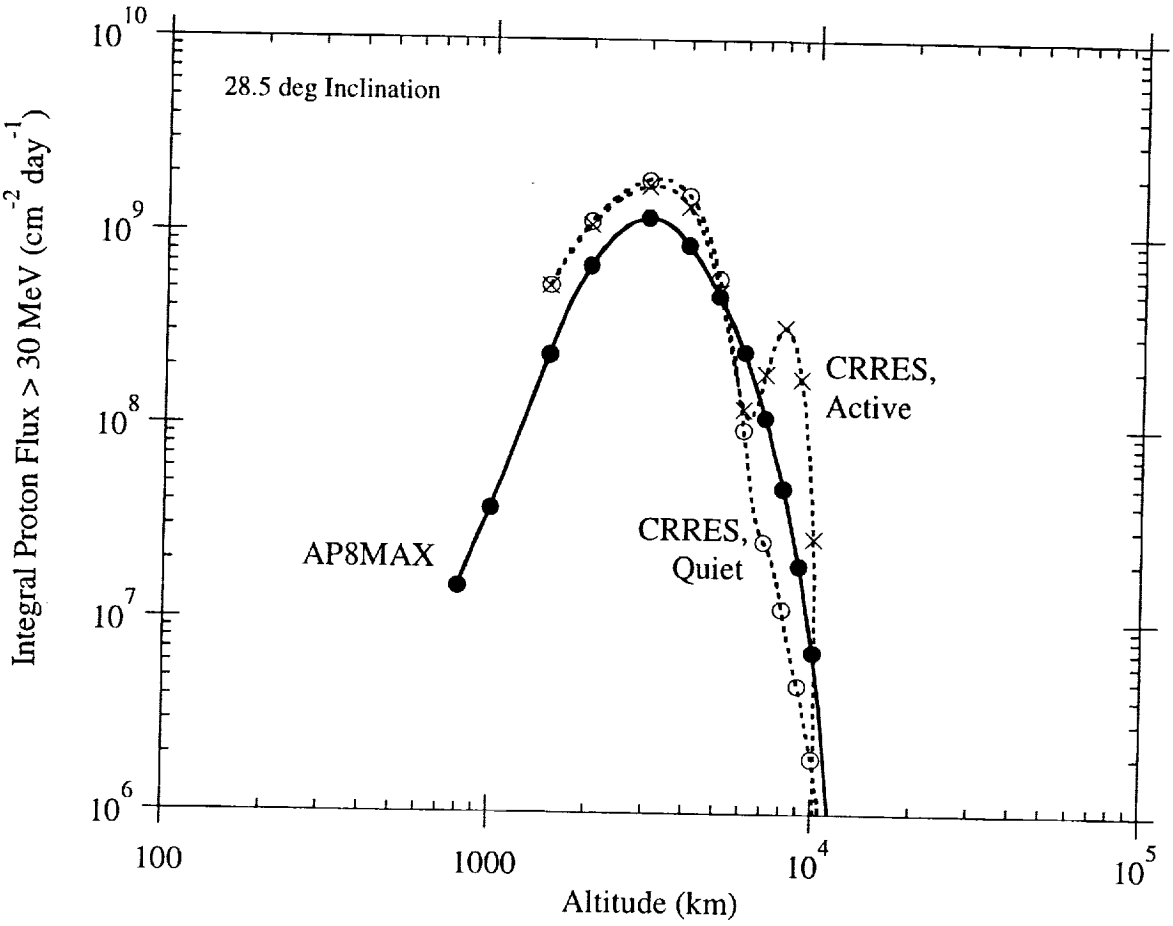

Fig. 4. Altitude dependence of proton flux > 30 MeV in inner radiation belt predicted using AP8MAX model and from PROTEL detector measurements on the CRRES satellite for quiet and active geomagnetic conditions.

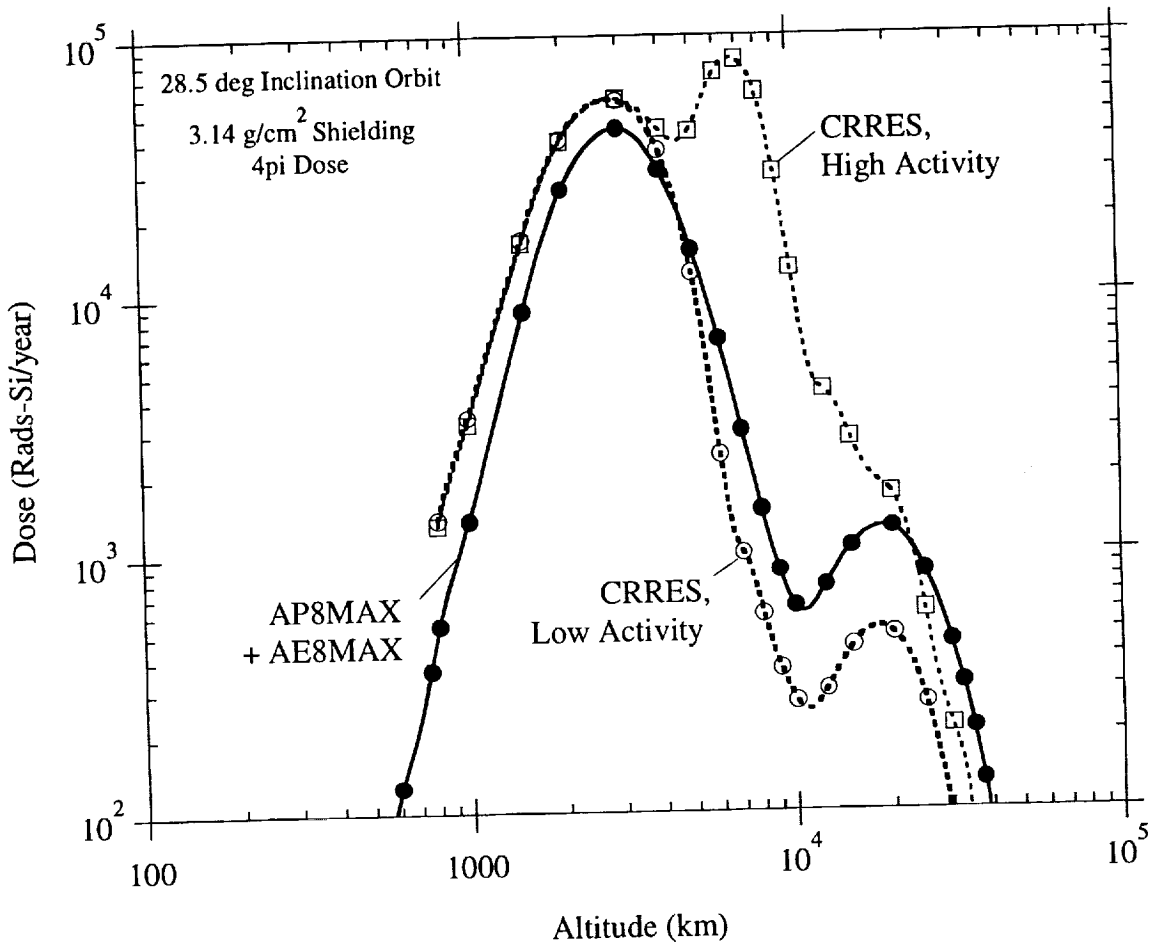

Fig. 5. Comparison of predicted dose vs. measured dose on CRRES for low and high geomagnetic activity levels.

underestimate the flux and dose for orbits passing through the outer region of the proton belt during transient periods of high magnetic activity.

Figure 6 shows the measured/model ratio for the flux and dose comparisons of Figs. 4 and 5 during quiet conditions, indicating approximate agreement using the two data sets. As also indicated in Fig. 6, these ratios join reasonably well with the NOAA-based ratios at lower (850 km) altitude.

3.2 Model Uncertainty Dependence on Solar Cycle

As indicated in Fig. 7, below about 1000 km the trapped proton flux is influenced by atmospheric losses and, therefore, atmospheric density changes due to solar heating. Comparisons of the NOAA data for integral proton fluxes above 16, 36, and 80 MeV at solar minimum and solar maximum with AP8MIN and AP8MAX predictions given in [20] show essentially the same model uncertainty at solar minimum and solar maximum in the 300-800 km altitude range. Also, model comparisons with activation measurements for various radioisotopes produced in material samples carried on LDEF suggest comparable uncertainties in the AP8MIN and AP8MAX models [24]. Therefore, we take the measured/predicted ratio of 2 ± 0.5 at low altitudes derived from the comparisons of Figs. 1 – 3 to be applicable to both AP8MIN and AP8MAX.

3.3 Model Uncertainty Dependence on Proton Energy

Both the NOAA and LDEF flight data and model comparisons indicate that the AP8 model uncertainty is independent of proton energy over a broad energy range. For example, the ratio of measured-to-predicted activities using AP8MIN and AP8MAX was approximately the same for material samples on LDEF (Fig. 8) despite the different proton energy thresholds (≥ 20 – 100 MeV) for the nuclear reactions producing the radioisotopes and the different amounts of shielding covering the samples. In one LDEF experiment, activation and absorbed dose measurements were made at the same location for shielding depths varying from about 1 to 19 g/cm^2 (aluminum equivalent), corresponding to the range of 28 to 150 MeV protons. The constant observed-to-predicted

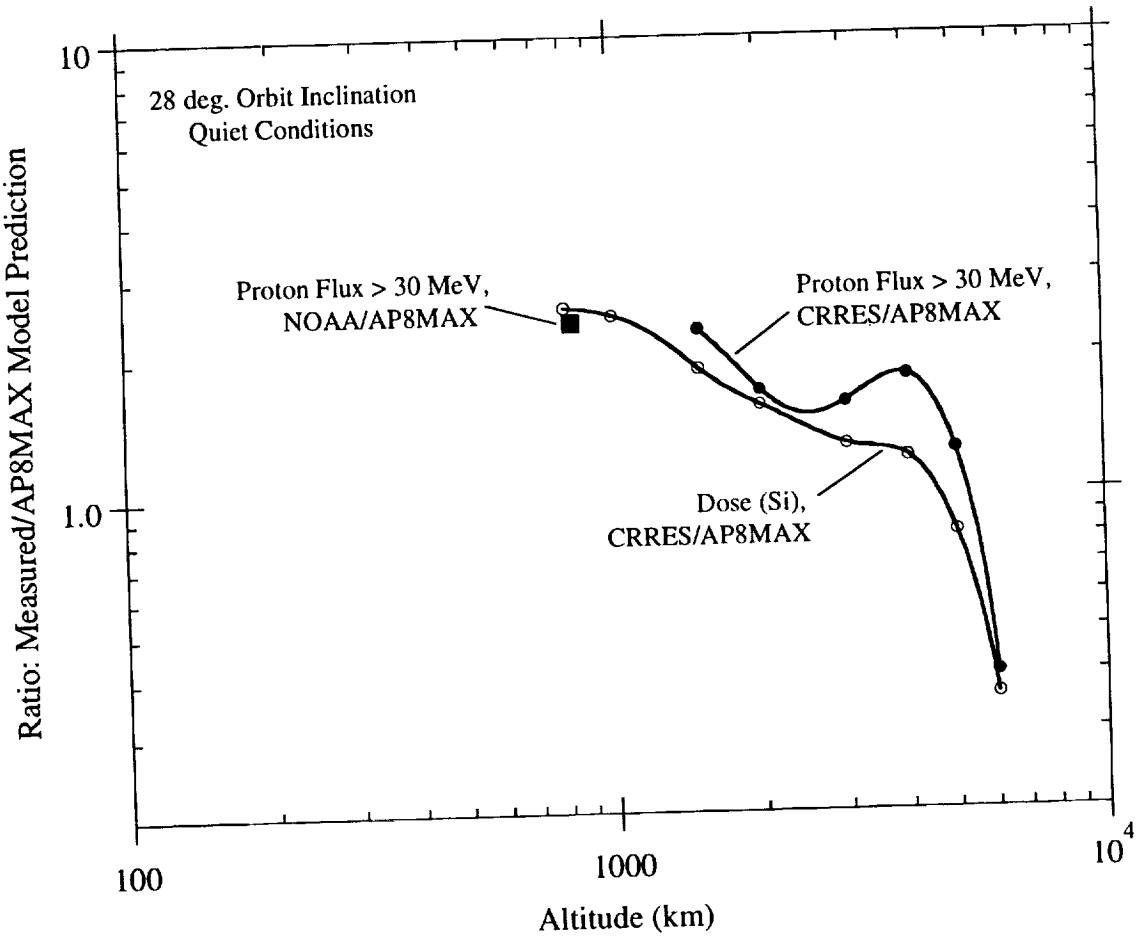

Fig. 6. Ratio of measured proton flux and dose to AP8MAX model predictions.

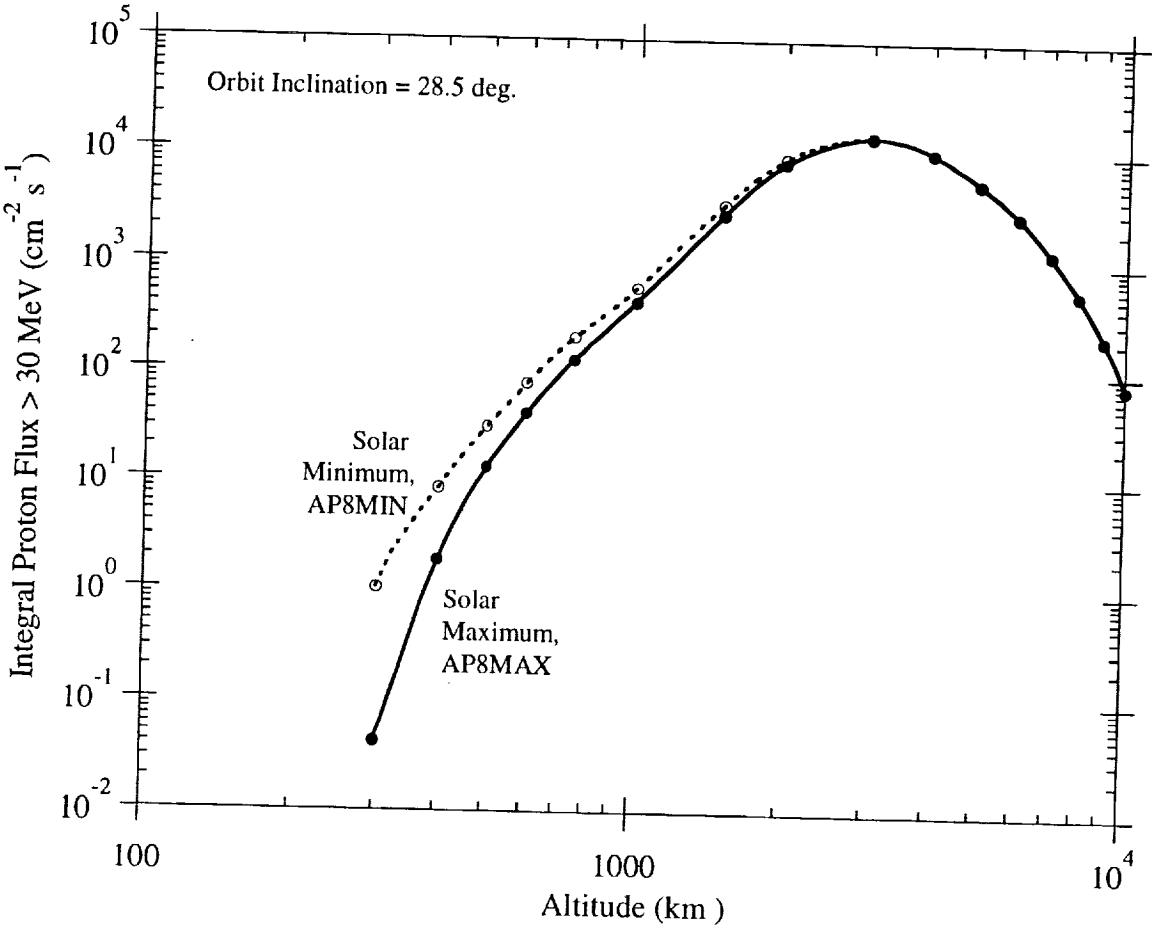

Fig. 7. Predicted influence of solar cycle on low altitude proton flux.

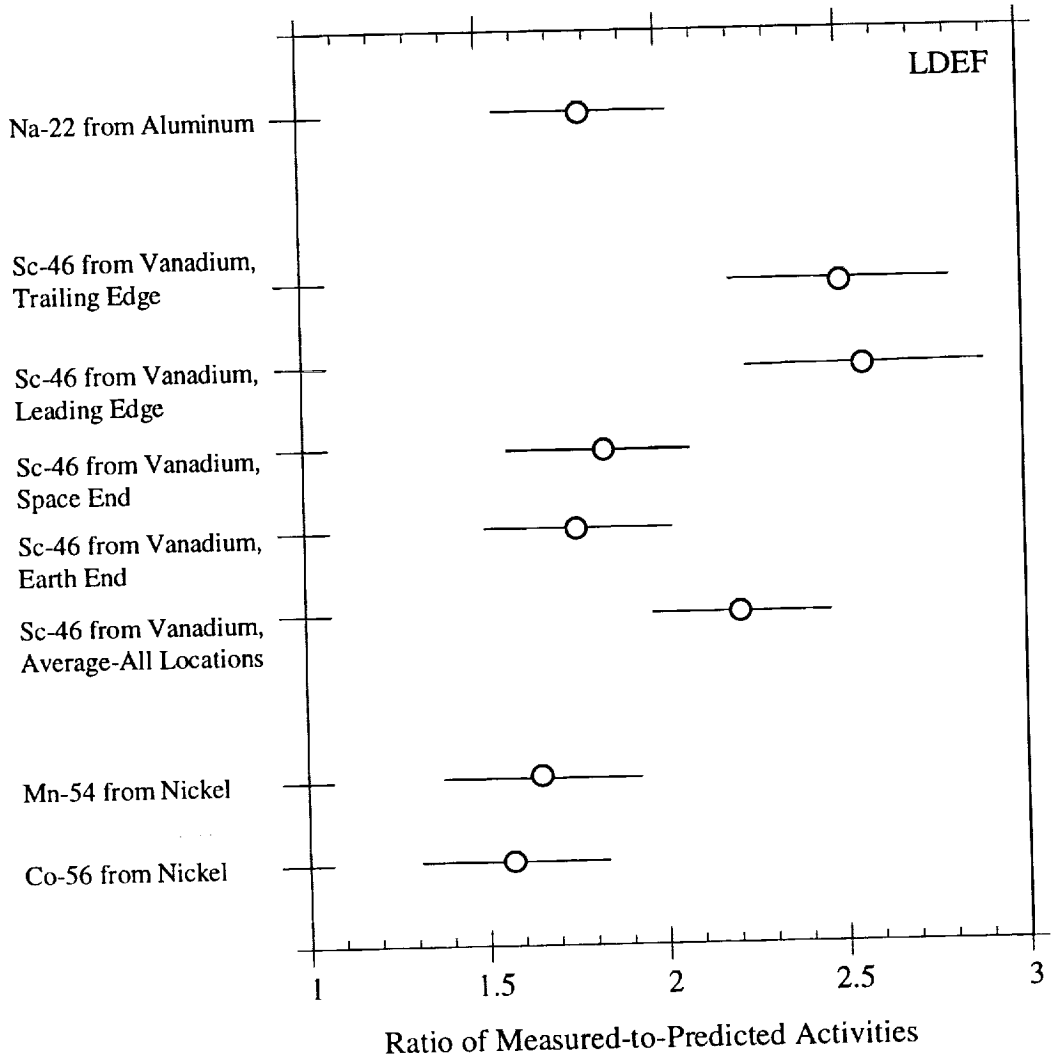

Fig. 8. Ratio of measured nuclear activation produced in material samples on LDEF satellite by protons to predicted activation using AP8 model, from [24].

ratio over this shielding range (shown in Fig. 9) indicates that the AP8 uncertainty is the same for proton energies from ● 30 to at least 150 MeV.

The NOAA data also indicates that the error in AP8 predictions is independent of proton energy for the measured energy range of 16 to 215 MeV. For example, at 850 km and solar minimum, the NOAA/AP8MIN integral proton flux ratios are 1.74, 1.70, and 1.85 for E > 16, 36, and 80 MeV, respectively. (These ratios are for a 28.5° inclination orbit, but the results are very similar for other inclinations)

3.4 Model Uncertainty Dependence on Radiation Effect

The conclusion above that the AP8 model uncertainty at low altitudes is independent of energy, at least in the energy range from about 15 MeV to several hundred MeV, has the important consequence that the uncertainty ratios shown earlier in Figs. 1 – 3 are expected to be independent of radiation effect. Thus, the same uncertainty factor associated with the trapped proton environment is applicable to predictions using AP8 for flux, dose, material activation, displacement damage, single event effects, etc.

3.5 Discussion

3.5.1 Scope

A complete review of AP8 model comparisons with flight observations quoted in the literature is not included here. This is mainly because such comparisons are commonly made in the context of approximate consistency checks between predictions and measurements. To definitively attribute such differences to uncertainties in the environment model requires an accurate treatment of other factors which can contribute to the uncertainty (such as a detailed analysis of shielding effects, accurate flight trajectory simulations, and, where applicable, accurate knowledge of the response function or cross section for the radiation effect measured). Analyses which delineate the different uncertainties are commonly not included in the reported model-data comparisons, so definitive, quantitative uncertainties related to the environment alone are often not available.

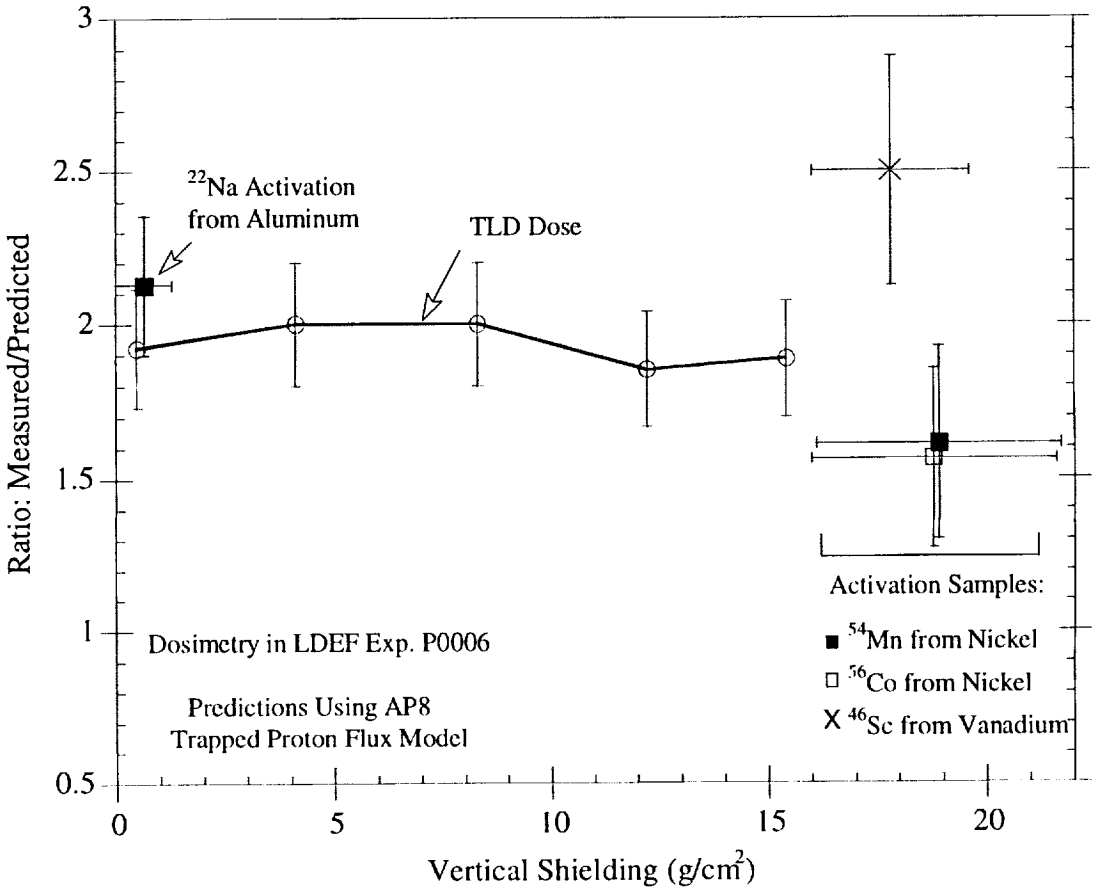

Fig. 9. Ratio of measured depth-dependent nuclear activation and dose from thermoluminescent dosimeters (TLDs) produced by protons on LDEF satellite to predictions using AP8 model, from [24].

3.5.2 Shuttle Data

One large flight data set not included here in the AP8 model comparisons is dose measurements that have been made on Shuttle flights. Such comparisons have been often reported in the literature; for example: the AP8 calculated dose was reported to be "nearly a factor of 2 higher" than dose measurements on Shuttle flight STS-63 (51.6°, 314 –395 km) [30]; for flight STS-60 (57°, 353 km), the average ratio was 1.82 [31], and in summarizing dose comparisons for a large number of Shuttle flights, it is stated in [32] that "based on Shuttle measurements both the AP8MIN and AP8MAX model dose calculations have consistently been higher by a factor of 1.8 – 2.0 when compared with TEPC (Tissue Equivalent Proportional Counter) measurements".

Thus, these reported model comparisons with Shuttle dose data indicate that AP8 overpredicts the trapped proton flux by about a factor of 2 at low altitudes, whereas the comparisons with other data sets made here (Figs. 1 – 3) show that AP8 underpredicts the flight data by a factor of about 2.

To investigate this apparent discrepancy, we have made calculations to compare with dose measurements made on some 60 Shuttle flights at low- (28.5°) and mid- (51.6°, 57°) inclinations. The calculations were compared with TLD dose measurements made at two locations on the Shuttle, taking into account the 3-D shielding distributions around the detectors; details of the calculations and comparisons are given in [4]. A summary of the results for 28.5° Shuttle flights are shown in Fig. 10 together with the comparisons for other flight data sets shown earlier in Fig. 1. The distinguishing feature of the Shuttle results is their variability, with the measured-to-predicted ratio varying from about 0.5 (in agreement with the literature values quoted above) to about 2 (in agreement with the value found here from comparisons with other flight data). The variability of the model-data comparison for Shuttle flights at mid-inclinations is similar [4].

There are several factors which may contribute to the variability of the Shuttle model-data comparisons. One is that AP8 is a static model applicable for predicting average fluxes over relatively long periods (6 months or so), whereas the duration of Shuttle flights is about one week, so AP8 cannot take into account such short term temporal variations. Also, in the low-altitude South Atlantic Anomaly region which dominates the Shuttle proton exposure, the trapped proton flux is anisotropic, so the

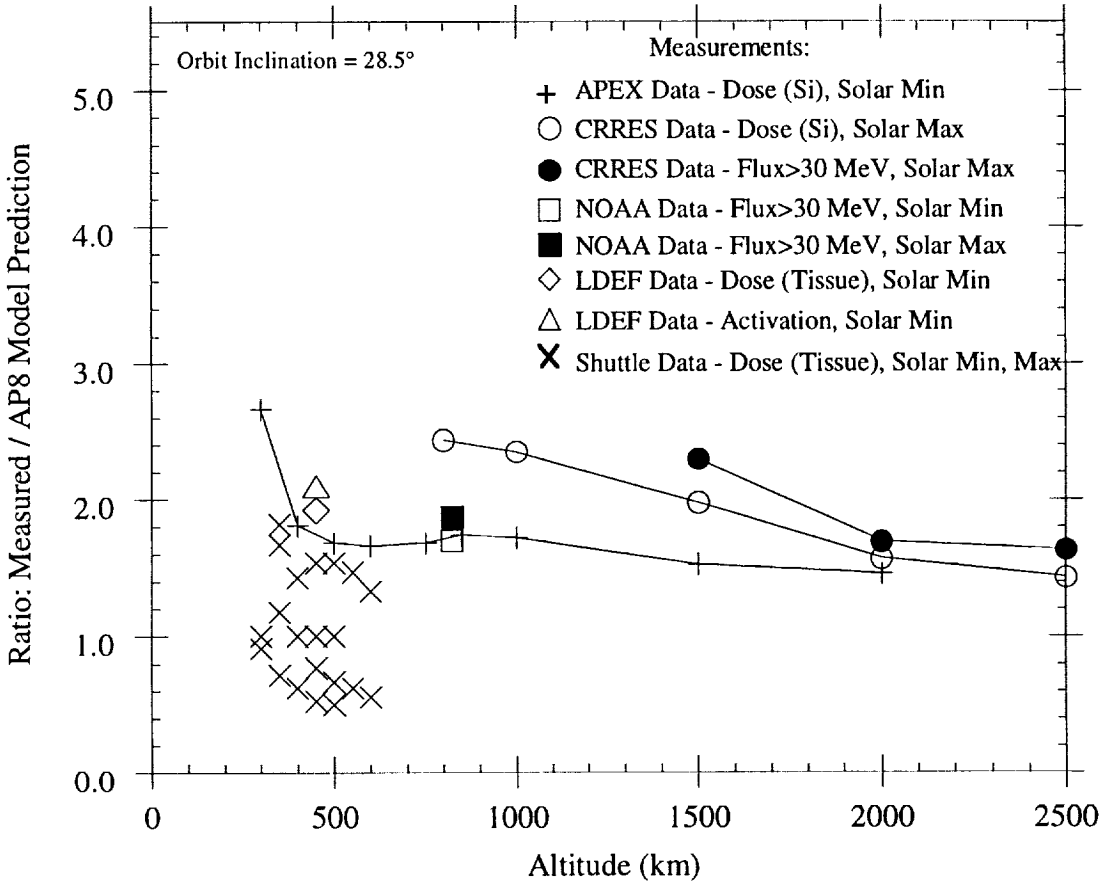

Fig. 10. Results of Fig. 1 with comparison of predicted and measured doses for Space Shuttle flights added.

incident flux and resulting dose can vary substantially with spacecraft altitude. For example, for LDEF (● 450 km, 28.5°), which was a gravity-gradient stabilized spacecraft with fixed attitude, the dose ratio on the West (trailing edge) of the spacecraft was measured to be 2.4 times the dose on the East (leading edge) of the spacecraft [23]. (This directionality of the proton flux was not taken into account in the Shuttle model predictions made here nor for the Shuttle ratios quoted above from the literature.)

Thus, application of AP8 model-data comparisons based on short duration Shuttle flights to long-term missions does not seem valid, and we have not included Shuttle measurements in the evaluation of AP8 model uncertainties here. In particular, the procedure used in [32] of reducing AP8 results by a factor of 1.8 based on Shuttle measurements in predicting long-term astronaut dose on the International Space Station seems inappropriate.

3.5.3 AP8 Model Limitations

The model uncertainties derived here are relevant, of course, only to AP8 applications that do not violate the model limitations. The major AP8 model application limitations are summarized below together with some references to related information.

Solar Cycle Dependence – The AP8 models provide fluxes at or near solar minimum or solar maximum conditions only, not the variations which occur during a solar cycle. The NOAA satellite data [19], covering 1.5 solar cycles, and reported long-term measurements on the MIR Space Station [33] provide guidance on estimating the solar cycle dependence of trapped protons.

Transients – The AP8 models are static in that they are most accurate in providing average fluxes for time periods of about 6 months or more. In particular, large temporal variations at high altitudes due to geomagnetic disturbances, such as observed during the CRRES mission [e.g., Figs. 4, 5), are not accounted for.

Directionality – The AP8 model provides only omnidirectional fluxes without any angular dependence. Models for generating directional proton spectra from AP8 omnidirectional spectra have been developed [34, 35] and tested against flight data [e.g., 23].

Energy Extrapolation – The AP8 model proton spectra below about 10 MeV are extrapolations of flight data, and the model uncertainty in this energy has not been evaluated here. An alternative to AP8 in determining proton spectra at very low energies is to use data from the S3-3 satellite, which provides spectra down to 80 kev for altitudes below 8200 km [36].

SAA Drift – Because of secular geomagnetic changes, the proton flux at low altitudes in the high intensity region of the South Atlantic Anomaly (SAA) region drifts westward at a rate of about 0.3° per year [37]. AP8 does not correctly predict the geographic location of fluxes in the SAA region because the magnetic fields that must be used to retrieve fluxes from the data base are those corresponding to the epoch of the flight data incorporated. However, as suggested in [37], the SAA drift can be accounted for approximately by simply shifting the AP8 predicted fluxes westward in longitude using the drift rate of 0.3°/yr and the time elapsed from the epochs corresponding to the AP8 data bases (1964 for AP8MIN, 1970 for AP8MAX). For altitudes below about 800 km the NOAA satellite data as incorporated in the NOAAPRO model [20] an be used to accurately treat the SAA drift.

3.6 Conclusions

3.6.1 Low Altitudes

The major finding from the AP8 trapped proton model comparisons with several sets and types (flux, dose, activation) of flight data is that for low-altitudes (below about 2000 km, where most of the flight data are available for comparison), the AP8 model underpredicts by about a factor of 2. By applying a factor of 2 correction to AP8 predicted proton fluxes, the model predictions are within about ☐ 25% of the flight data.

Another important conclusion is that this simple factor of 2 model correction is approximately independent of solar cycle (i.e., the same for AP8MIN and AP8MAX) and independent of proton energy (at least above about 15 MeV, where the model has been checked here against flight data). This constant uncertainty with energy has the important consequence that we expect the same factor of 2 correction to apply not only to the model predicted fluxes but to radiation effects estimates (dose, displacement damage, single

event effects, activation, etc.) made using the model fluxes. For example, the factor of 2 correction would be applicable to predicted single event upsets induced by trapped protons regardless of the threshold or energy dependence of the upset cross section.

A caveat for the constant uncertainty vs. energy conclusion is that data comparisons below about 15 MeV have not been made here. Thus, we cannot give an uncertainty factor for AP8 applications where < 15 MeV protons are important, such as solar cell damage predictions. (We note, however, that predictions of solar cell degradation using AP8 are in very good agreement with measurements made on the APEX satellite for some 15 different solar cell technologies [38]).

The factor of 2 correction factor derived here applies, of course, only for situations where the AP8 model itself is used within the limitations summarized above in Sec. 3.5.3 In particular, the correction factor is not generally applicable for short duration flights such as the Space Shuttle.

3.6.2 High Altitudes

Fewer flight data sets are available for testing the accuracy of the AP8 model at higher (> 2000 km) altitudes. Based on proton flux and dose data taken on the CRRES mission, AP8 continues to underestimate to altitudes just past the peak intensity of the proton belt and then overestimates in the outer regions of the belt (Figs. 4-6). The CRRES data show that the outer regions of the belt are subject to temporary large enhancements due to geomagnetic storms, and the AP8 model may grossly underestimate proton fluxes in this region during and some months after such disturbances.

4. Trapped Electron Model Uncertainties

4.1 Model-Data Comparisons

4.1.1 Low-Altitude, Thin-shielding Dose Comparisons

As noted in Sec. 2.1.2, one of the dosimeters on the APEX satellite consisted of a silicon detector beneath a thin (4.3 mils, or 0.029 g/cm^2) slab of aluminum and sensitive to electrons above 150 keV and protons above 5 MeV. For such thin shielding, the dose is dominated by electrons, so data from this dosimeter can be used to check the accuracy of the AE8MIN model for predicting spacecraft near-surface dose levels in the low-altitude range where the APEX data are applicable (300-2000 km).

Figures 11 and 12 show the APEX/AE8MIN dose ratio for circular orbits as a function of altitude for selected inclinations and as a function of inclination for selected altitudes, respectively. The ratios can be considered in three categories: (a) For inclinations below about 40° and altitudes below about 750 km, the orbits are essentially below the radiation belts and the electron dose levels are low. Below about 20° and 500 km, the trapped electron dose is expected to be below the galactic cosmic-ray dose. (The cosmic-ray background has been subtracted from the APEX dose or part of the data analysis [16].) Thus, while AE8MIN underprediction is large in this region, the practical importance is lessened because of the low dose levels. (b) For low altitudes (below about 750 km) and high inclinations (above about 40°), the dose is due mainly to exposure in the "horns" of the outer zone electrons which reach low altitudes at high latitudes. In this region, AE8MIN underpredicts by about a factor of 2 (see Fig. 12). The dose in this region is sensitive to outer zone intensity fluctuations caused by magnetic disturbances, so the model uncertainty depends on the magnetic activity level. (c) For altitudes above about 1500 km at low (< 40°) inclinations, and altitudes above about 750 km for high (> 40°) inclinations, the dose is due to electrons in the inner radiation belt, and AE8MIN overpredicts the dose by about a factor of 2 at low inclinations and a factor of 1.5 at high inclinations.

The results of Figs. 11 and 12 are based on the average magnetic activity level during the APEX mission. To indicate the sensitivity of these results to magnetic activity, in Fig. 13 the APEX dose for high magnetic activity periods (corresponding to the dose

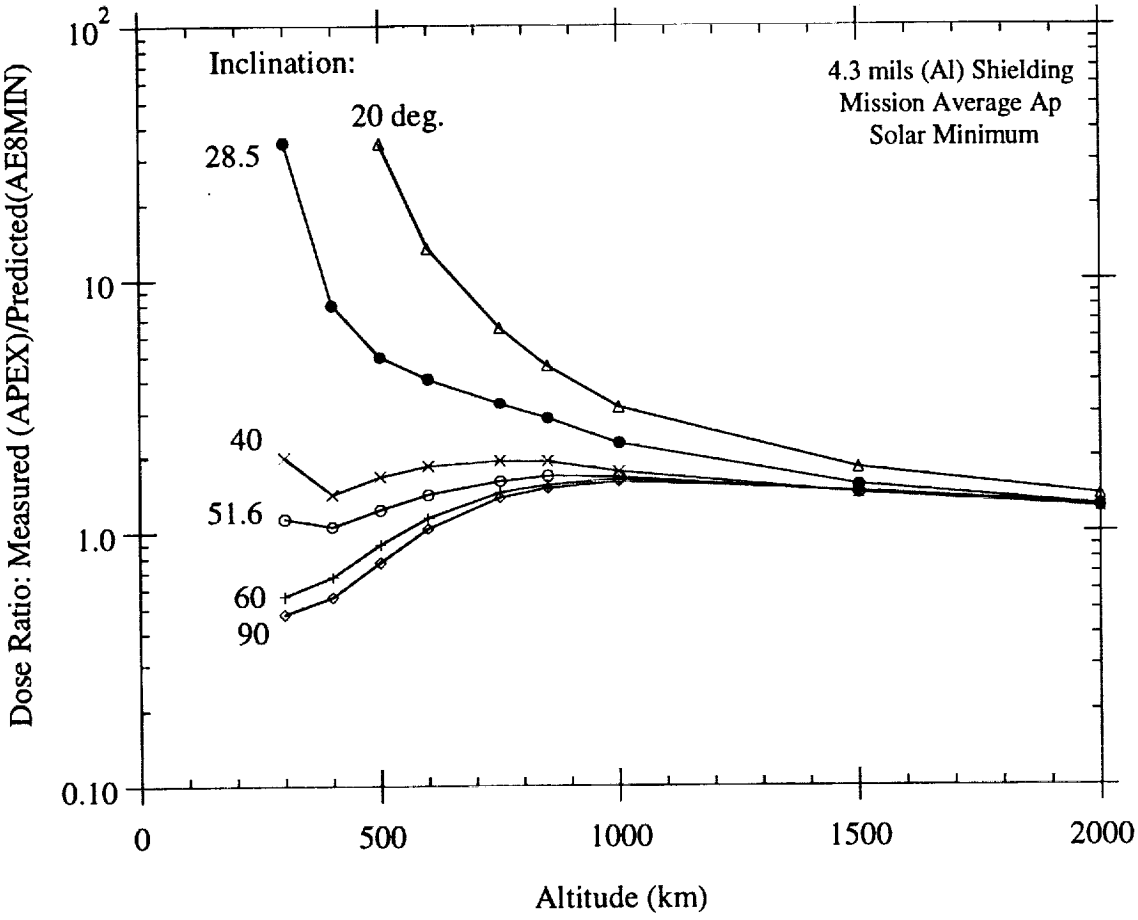

Fig. 11. Comparison of dose at low altitudes behind thin shielding (4.3 mils of aluminum) measured on APEX satellite with predictions using AE8MIN model.

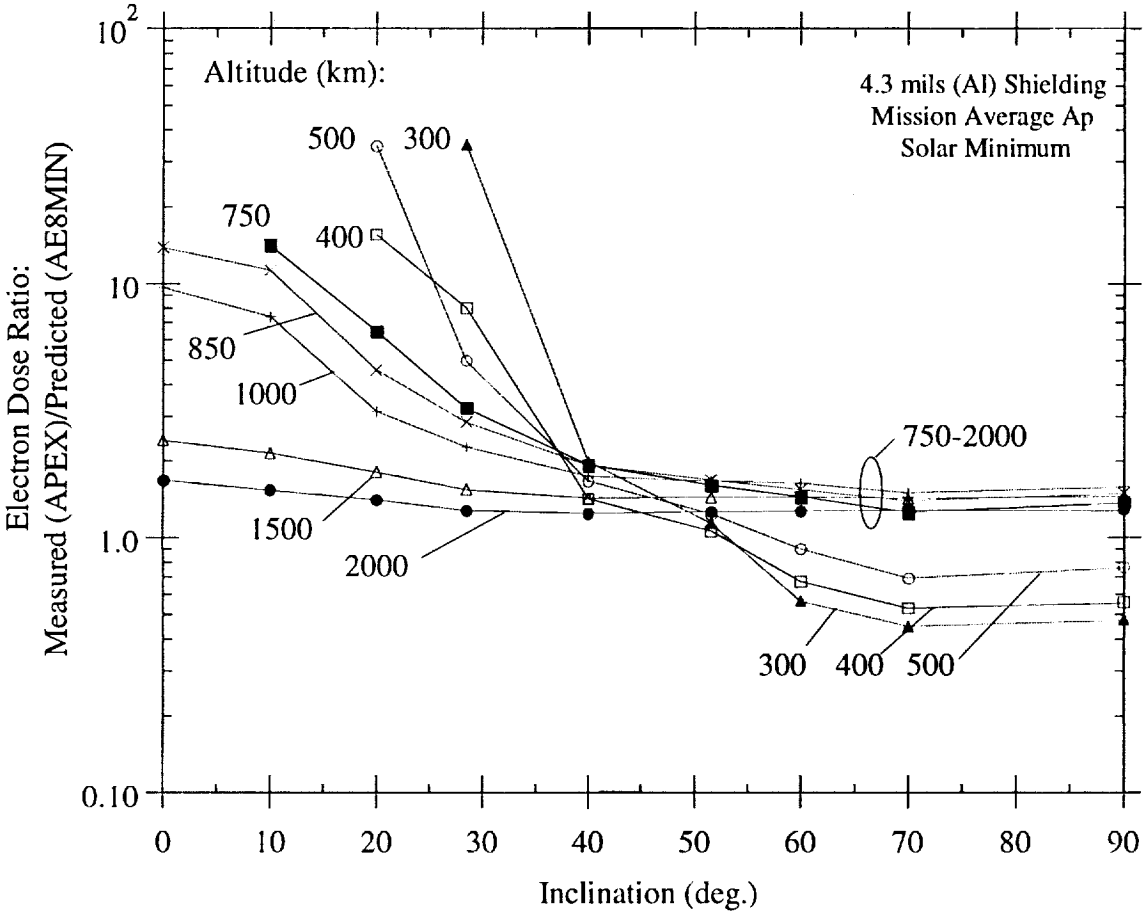

Fig. 12. Results of Fig. 11 plotted vs. orbit inclination.

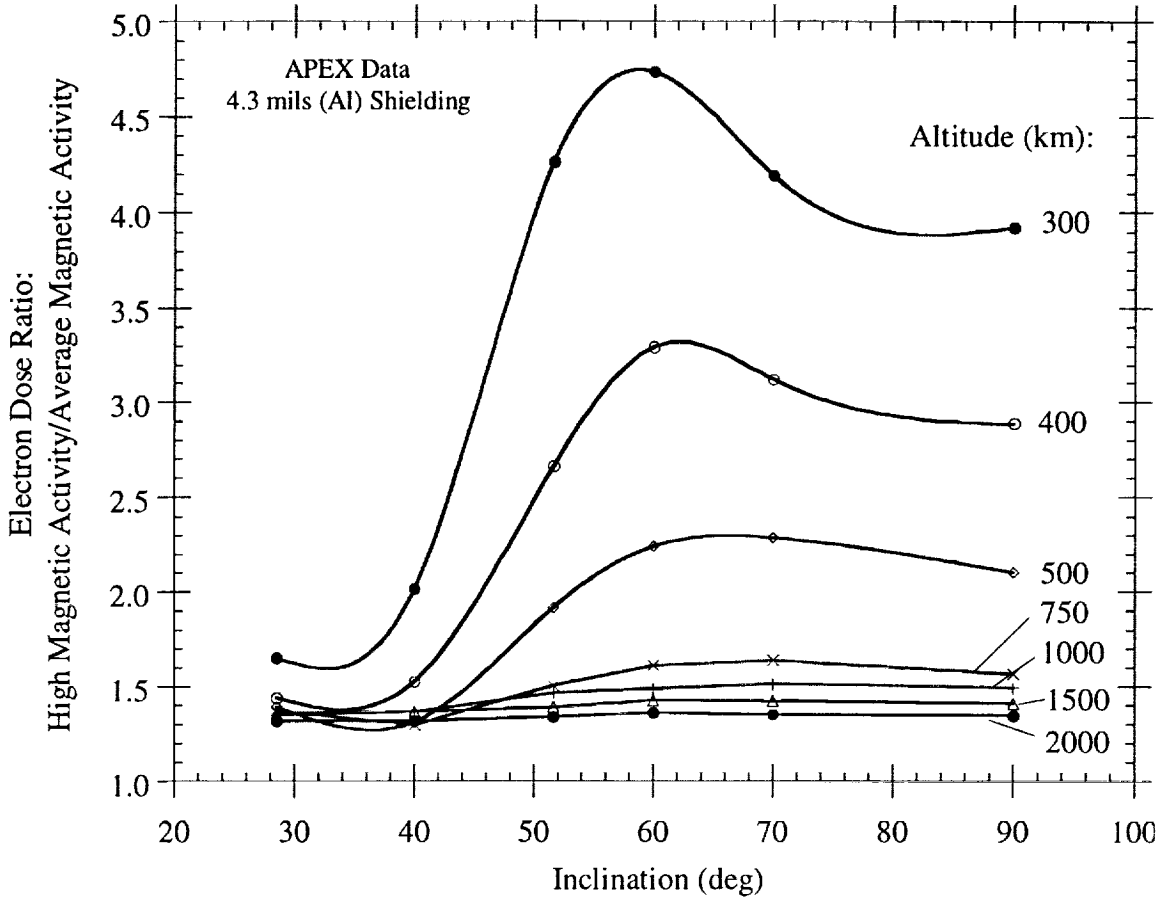

Fig. 13. Comparison of low-altitude, thin-shielding dose from electrons measured on APEX for high and mission average magnetic activity levels.

measured in the Ap_{15} index range of 20 to 25) is compared with the mission average dose. This illustrates the large variations which can occur for low altitude (< 750 km), high-inclination (> 40°) orbits where exposure is dominated by the outer zone electron horns, and also indicates that the electron flux at the inner belt inner edge is fairly stable. As an approximate upper limit for AEMIN prediction uncertainty during periods of high magnetic activity, the ratios of Figs. 11 or 12 should be multiplied by the ratios in Fig. 13.

As further tests of the accuracy of AE8 in predicting thin-shielding dose from electrons, we have compared predictions with depth-dose measurements made on several low-altitude spacecraft using thermoluminescent dosimeters. From these results, given in [4], we have extracted measured/predicted ratios corresponding to the APEX thinnest shielding (4.3 mils aluminum) and compared them with the ratios based on APEX data as a consistency check. This comparison is shown in Fig. 14, where the horizontal bars represent the altitude range during the mission, and the vertical bars represent the spread in the data where multiple data sets were available. Shown are ratios from measurements on Cosmos-2044 (82.3°, 216 - 294 km, solar max), Cosmos-1887 (62.8°, 224 - 406 km, solar min), Photon-8 (62.8°, 220 - 359 km, midway between solar max and solar min), Mir Space Station (51.6°, 400 km, solar max), LDEF (28.5°, 319 - 479 km, mainly solar min), and Shuttle Flight STS - 46 (28.5°, 420 - 520 km, midway between solar min and solar max). Two ratios are shown for Mir: "active", from measurements about 3 months after the intense magnetic disturbance of March 1991, and "quiet", from measurements made during a period of low magnetic activity in 1997.

As indicated by Fig. 14, the measured/predicted electron dose ratios for these spacecraft are generally consistent with the APEX ratios but the ratio range is broad, from about 0.5 - 2 (excluding the "Mir active" ratio, which is about 5). The Russian spacecraft are in the altitude-inclination regime where, as indicated by Fig. 13, the dose levels are sensitive to magnetic activity. Also, it is important to note that, except for LDEF, the measurements were made over short time periods (a few weeks) and that temporal variations on this time scale are not accounted for by the static AE8 model. Given these model limitations, and that the comparisons shown are for different times during the solar cycle, the data/model ratio variation shown in Fig. 14 is not unexpected.

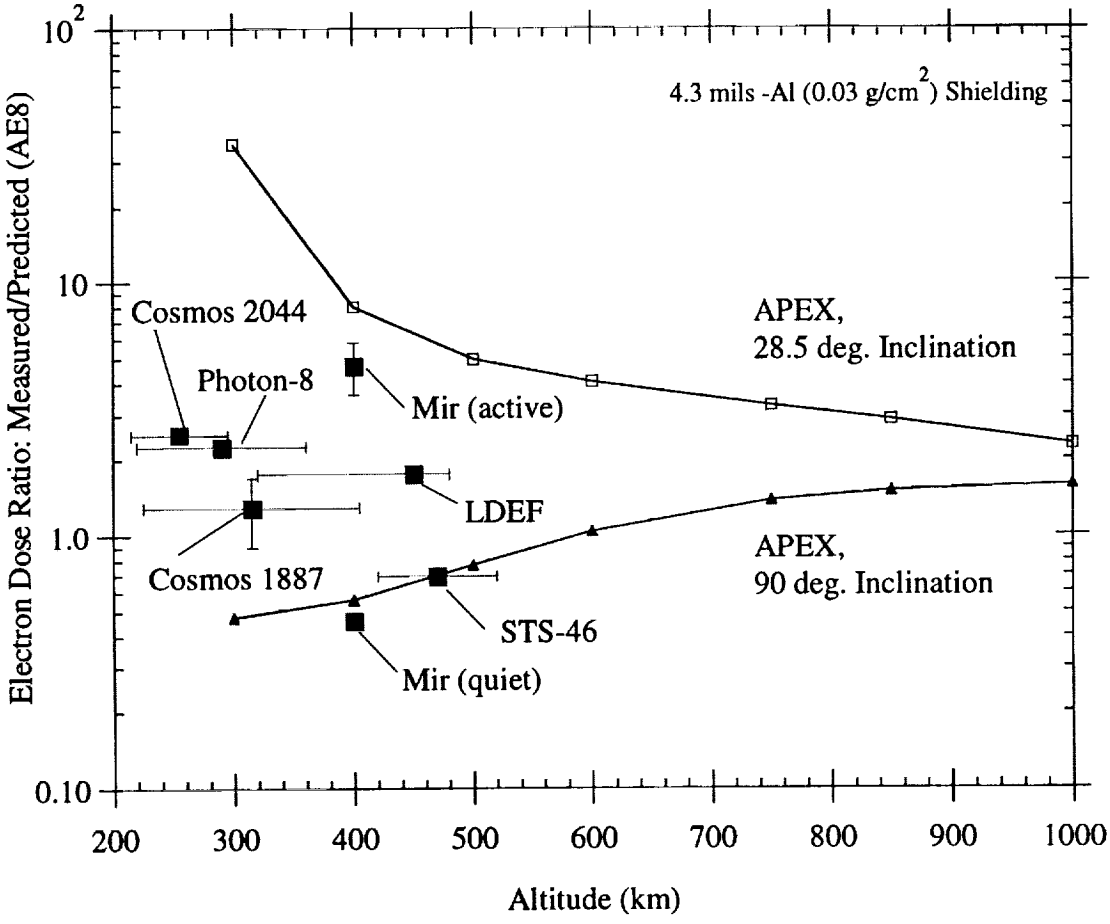

Fig. 14. Comparison of various sets of flight data for low-altitude, thin-shielding dose from electrons with predicted doses using AE8 trapped electron model.

4.1.2 High Altitude Comparisons – Quiet times

Figure 15 shows a dose comparison predicted using AE8MAX and measured on CRRES during quiet conditions, i.e., the period of low geomagnetic activity during the mission before the March 1991 event. The CRRES results, calculated using the CRRESRAD software utility, are from the detector with thinnest shielding (82.5 mils aluminum, 0.57 g/cm^2) and the low LET data, which measures essentially the dose from electrons. For these comparisons, the CRRES hemispherical detector data have been multiplied by two to compare with the AE8MAX doses calculated for 4π solid angle incidence on an aluminum sphere of 0.57 g/cm^2 radius.

Figure 16 shows the AE8MAX/CRRESRAD dose ratio for the curves in Fig. 15. (Note that here we show the model/data ratio, whereas in previous graphs data/model ratios have been shown). Fig. 16 shows: (a) in the peak and outer edge of the inner belt ($\approx$ 2,000 – 5,000 km), AE8MAX overpredicts by about a factor of three, (b) in the low dose 'slot' region between the inner and outer belts (5,000 – 10,000 km), AE8MAX overpredicts by as much as a factor of 50, (c) in the peak region of the outer belt, AE8MAX overpredicts by a factor of 5 – 10, and (d) in the outer regions of the outer belt, AE8MAX overpredicts by a factor of 10 – 100.

4.1.3 High Altitude Comparisons – High Activity

Data from the CRRES mission taken after the extremely large geomagnetic disturbance and solar particle event of March 1991 provide what is probably a practical upper limit for temporal enhancements to the trapped electron populations. Thus, comparison of these data with AE8, which is a static model and does not account for fluctuations due to geomagnetic storms, provides a bound on AE8 uncertainty related to geomagnetic activity.

Figure 17 shows the AE8MAX and CRRES low activity dose curves of Fig. 15 with the average dose measurements during the 6-month observation period after the March 91 storm ("CRRES, High Activity" curve). These results show that such a large disturbance enhances the electron dose down to altitudes corresponding to the peak of the inner belt, with increases of about two orders-of-magnitude in the slot region and one order-of-magnitude in the peak region of the outer belt. However, the static AE8MAX

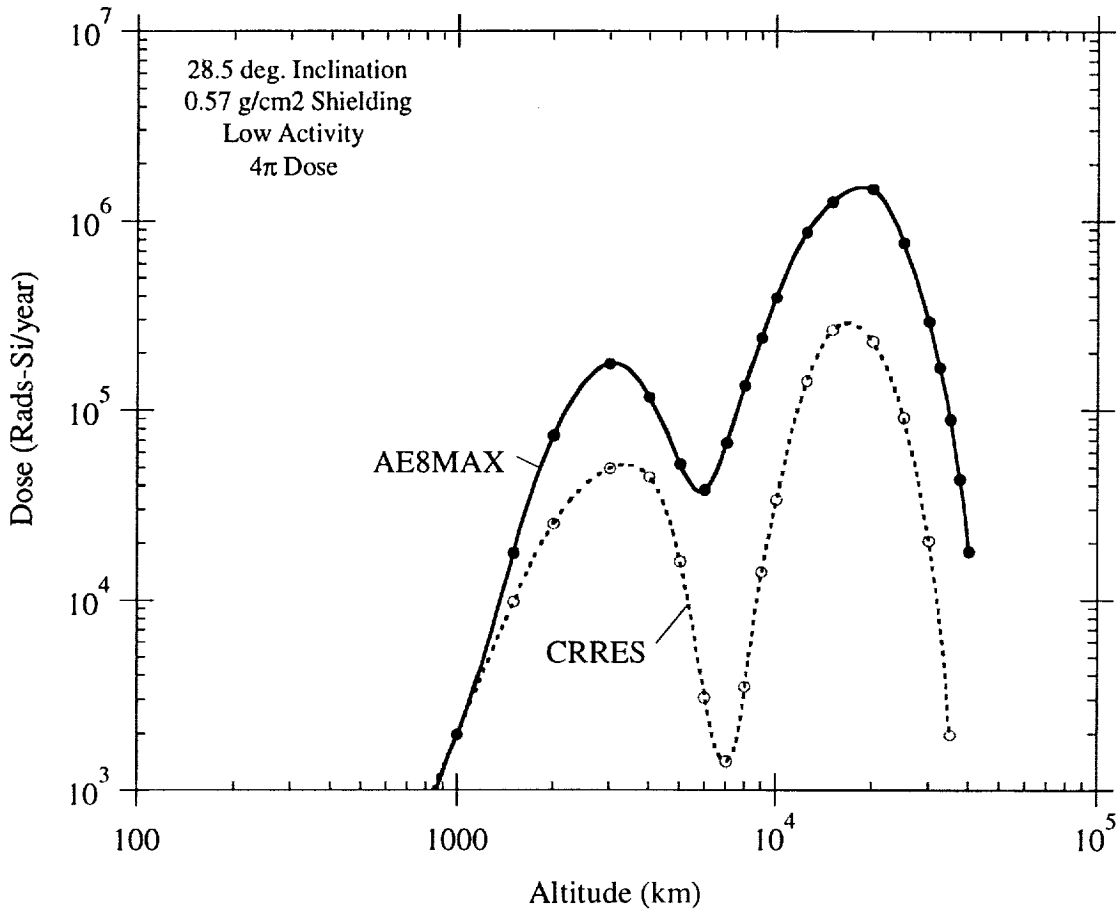

Fig. 15. Comparison of electron dose based on CRRES satellite measurements with predictions using AE8MAX model – for low magnetic activity conditions.

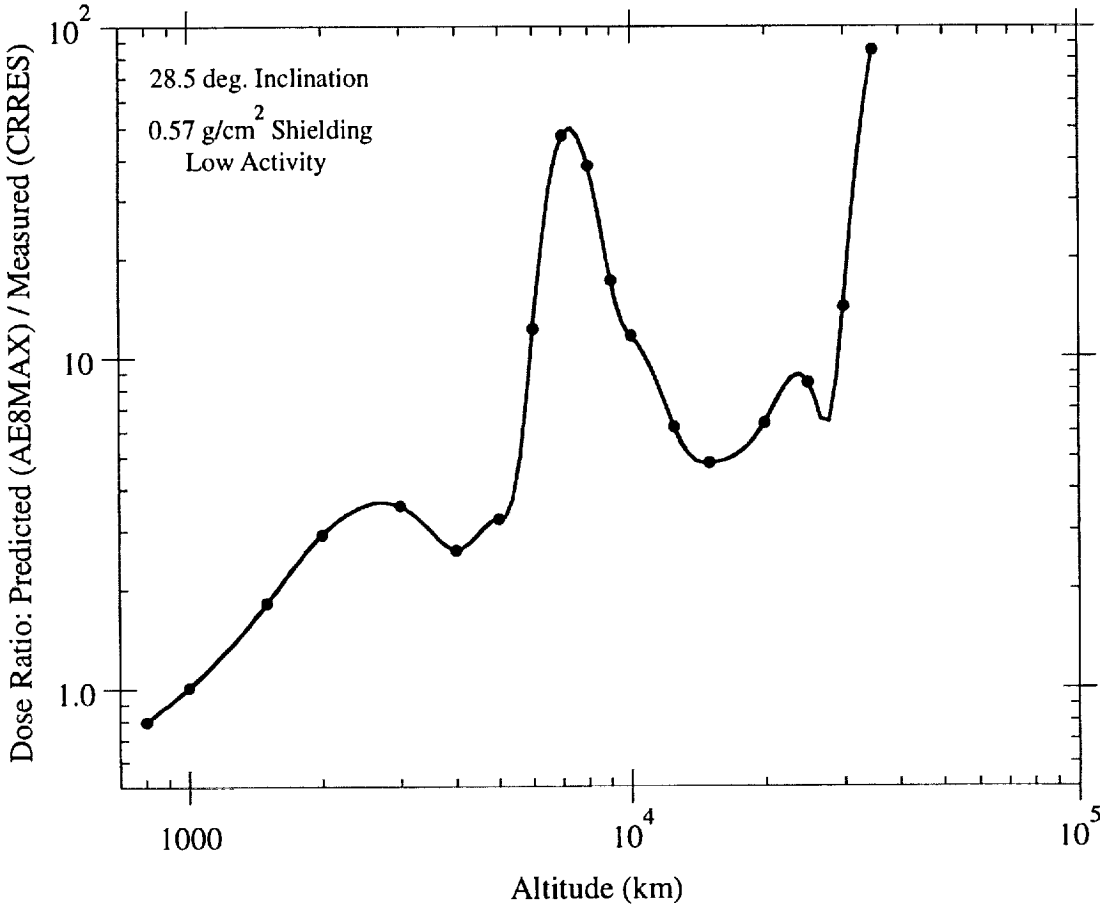

Fig. 16. Ratio of predicted electron dose using AE8MAX to dose from CRRES satellite measurements for low magnetic activity conditions.

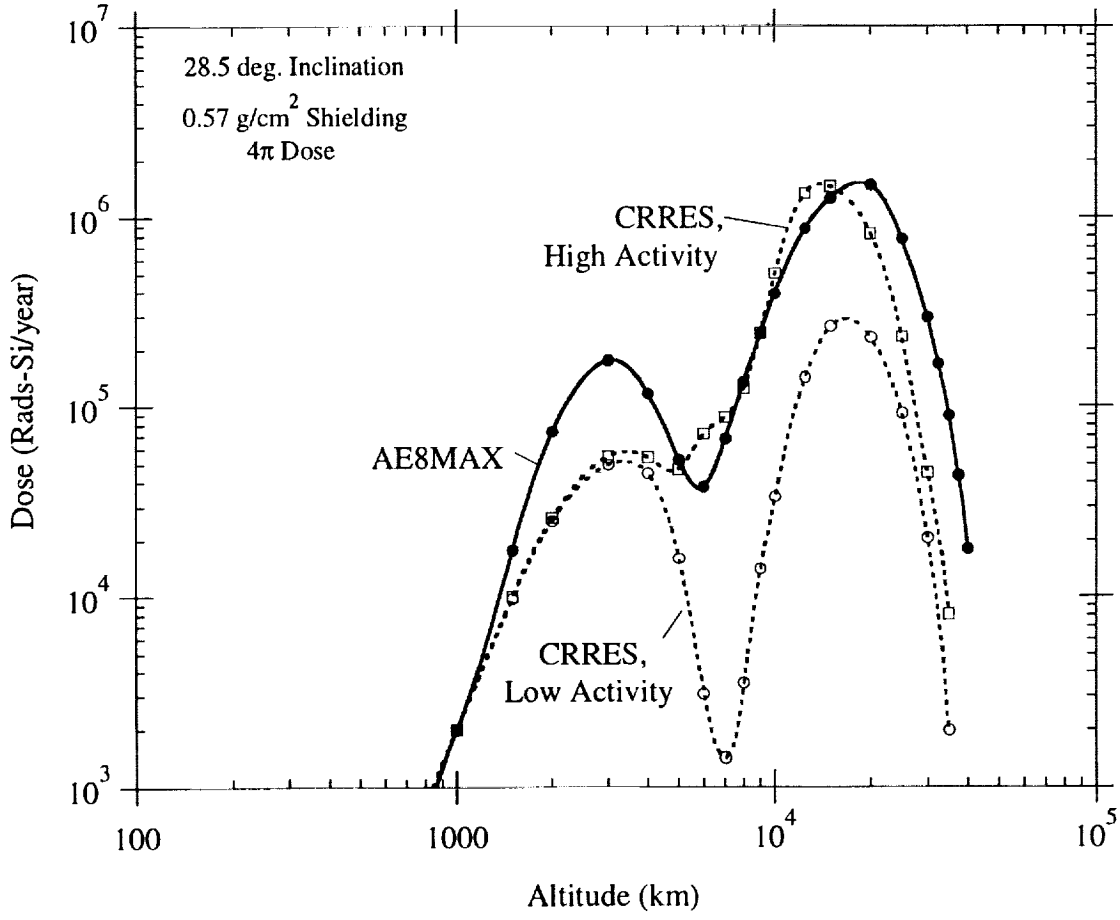

Fig. 17. Comparison of electron dose based on CRRES satellite measurements for low and high magnetic activity conditions with predictions using AE8MAX model.

model overestimates the dose levels for quiet conditions by such a large amount that the model results are not appreciably exceeded during these extremely high activity conditions, and the model doses are still overestimates in the inner belt (by a factor of about 3 near the peak) and for the outer edge of the outer belt (by a factor of about 10 or more).

Figure 18 compares the AE8MAX electron flux > 1.2 MeV with the outer belt fluxes measured by the CRRES HEEF detector. The HEEF data are given for different levels of magnetic activity as measured by the Ap_{15} magnetic index – i.e., as if the whole mission was during the indicated activity levels. The basic features of this flux comparison are the same as the dose comparison of Fig. 17 – i.e., AE8MAX predictions are comparable to the flux or dose observed for the very highest levels of magnetic activity in the peak region of the outer belt and significantly higher at the outer edge.

The outer belt ESA-SEE1 electron model is for solar minimum and based on CRRES mission average electron measurements (high and low activity). A comparison of AE8MIN and AE8MAX with the ESA-SEE1 data base in terms of the altitude-dependent electron flux > 1.2 MeV is given in Fig. 19. The ESA-SEE1 flux, which as discussed in Sec. 2.1.1 is based on the CRRES MEA detector with added energy spectra extrapolations, is somewhat higher than the flux from the HEEF detector shown in Fig. 18 – i.e., the mission average ESA-SEE1 flux is comparable to the HEEF flux for the highest activity level in Fig. 18.

4.2 Discussion

Evaluation of the uncertainties associated with the AE8 trapped electron model is complicated by several factors – namely: (a) there are large transient fluctuations caused by geomagnetic disturbances and solar particle event injection, whereas AE8 is a long-term (six months or so) average flux model not capable of predicting trapped electron dynamics; (b) there are several trapped electron source regions (polar horns, inner belt, outer belt), and orbits of interest commonly pass through multiple source regions, which complicates the derivation of simple guidelines on quantitative model uncertainties for orbit-average environments and effects; and, (c) the flight data currently available for checking the model accuracy is very limited.

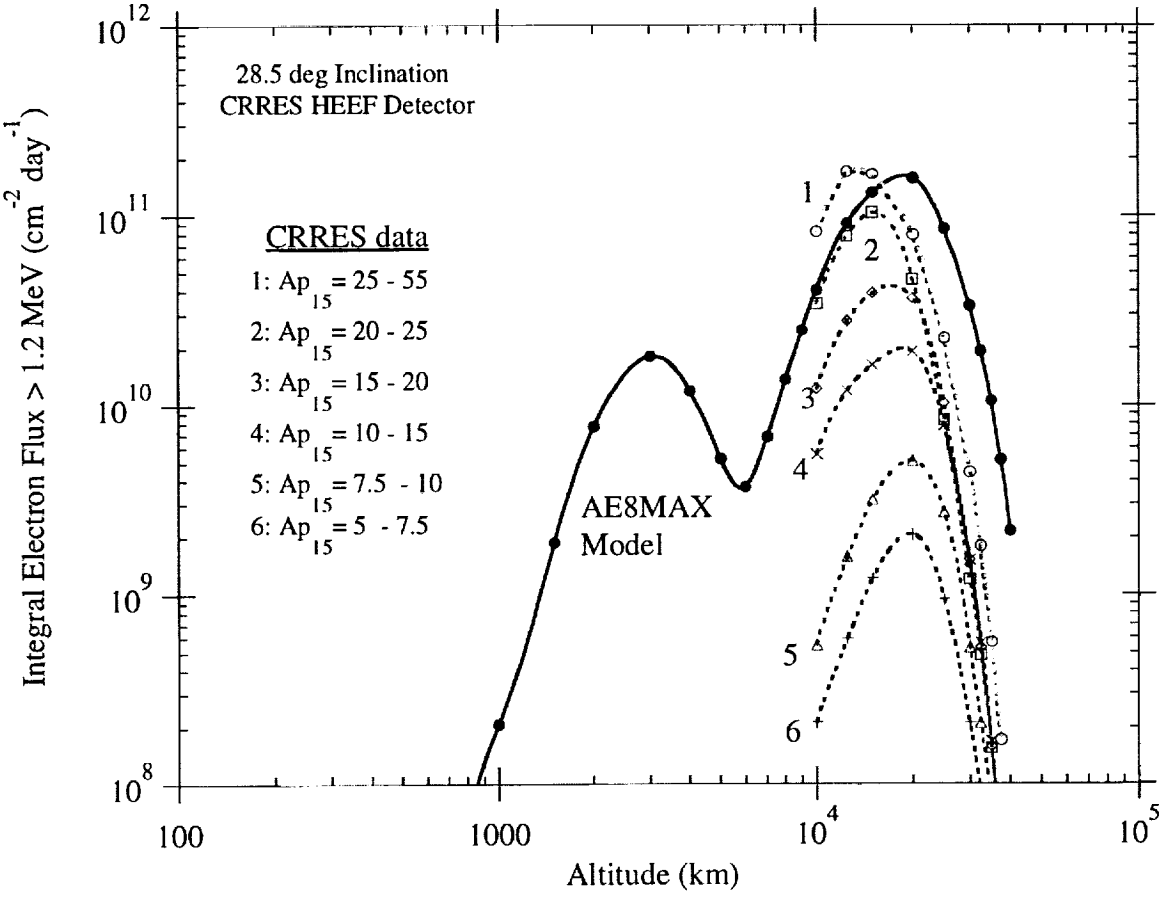

Fig. 18. Comparison of electron flux from CRRES satellite measurements for various magnetic activity levels with predictions using AE8MAX model.

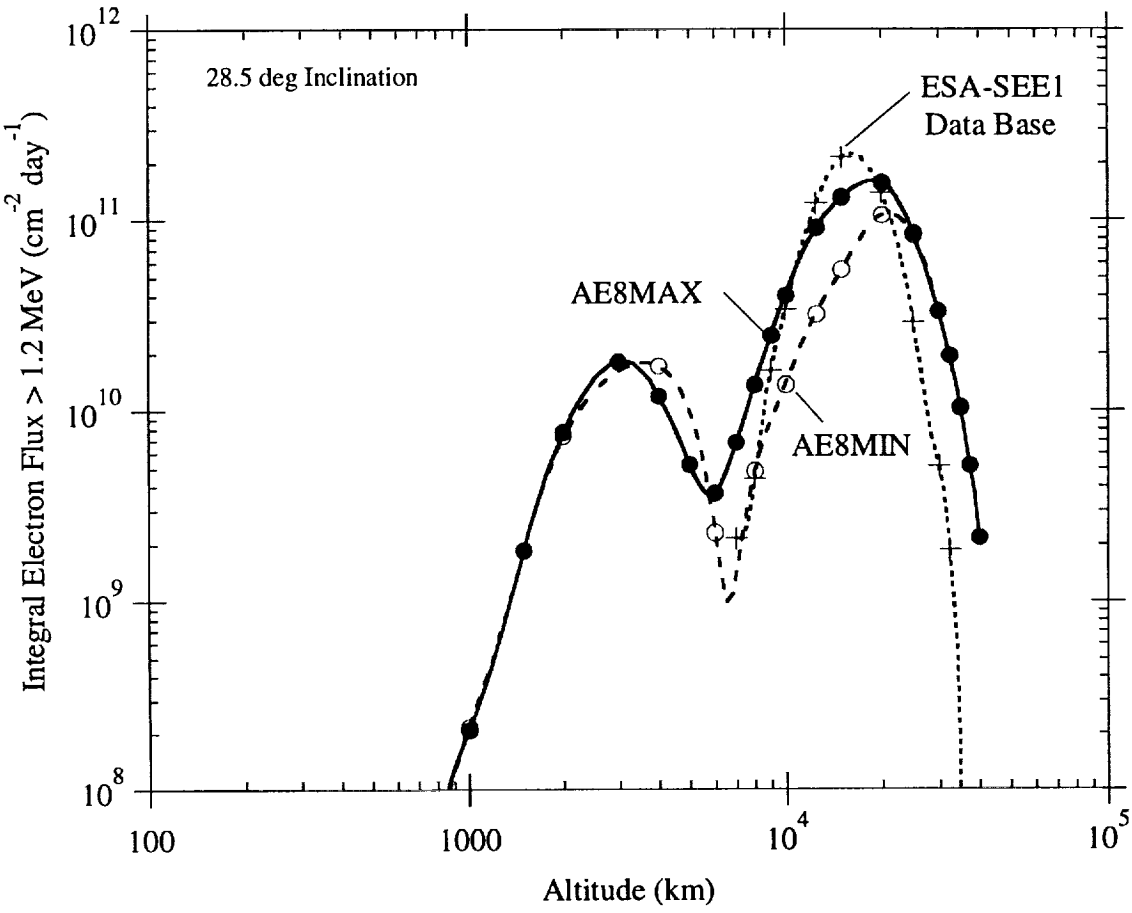

Fig. 19. Comparison of electron flux from ESA-SEE1 data base [43] based on CRRES satellite measurements for mission average magnetic activity and energy spectra extrapolations with AE8MIN and AE8MAX model predictions.

Despite these difficulties, it is clear from the comparisons here that the AE8 model substantially overestimates the trapped electron intensity in both the inner and outer belts. The overestimate for the inner belt shown here (Fig. 17) is confirmed by the recent study of Abel, et al. [39] in which data from six satellites covering the period 1966 – 1991 were analyzed. They found a continuous decline in inner zone electrons with energies > 1 MeV, and attribute this to the decay of remnants from upper atmospheric nuclear detonations carried out in the late 1950s and early 1960s. For electron energies below 1 MeV, they found large short-term fluctuations occur due to inward radial diffusion of outer zone electron disturbances from geomagnetic storms, and there are variations due to solar cycle effects.

It is clear from the outer belt dose comparison (e.g., Fig. 17) that AE8 fluxes significantly overestimate the dose at geosynchronous altitudes, as has been pointed out several places in the literature [e.g., 40, 41]. We calculate the AE8MAX/CRRES dose ratio (0.57 g/cm^2 shielding) for a geostationary orbit (0° inclination; 35,800 km altitude) to be 56 for low magnetic activity and 10 for high activity. An AE8/measured dose ratio of 12 for similar (0.69 g/cm^2) shielding has been observed for Molniya – type orbits [42].

The AE8 model comparisons here with the CRRES data for low (or nominal) geomagnetic activity and high activity indicate the regions which are significantly affected by enhanced fluxes following large geomagnetic disturbances. To account for dose variations due to such disturbances in estimating the total dose for a mission, making estimates using the "high activity" results alone from CRRES for the whole mission would be overly conservative since these data represent a 6-month average after the largest disturbances of this type ever observed. There is some evidence that disturbances of the magnitude observed during the CRRES mission in 1991 (i.e., large enough to create a third belt) may have also occurred in 1958 [43], in 1963 [44] and in 1986 [45], or roughly one such disturbance per 11-year solar cycle. Thus, a reasonable assumption would be one such disturbance during a 5- or 10-year mission with the extreme dose due to magnetic activity fluctuations based on one-year of CRRES high activity and the remaining years using CRRES low activity results. The point here is that for practical total dose mission estimates, the mission-average difference between high-activity and

low-activity dose estimates will typically be substantially less than the high-activity and low-activity CRRES curves shown here (e.g., Fig. 17).

We have not addressed uncertainties in the spectral shape of the AE8 model electron fluxes. Above a few MeV, the accuracy of the AE8 model spectra are suspect because of uncertainties in detector efficiencies and background corrections for the flight data incorporated in the model [14]. This is consistent with AE8 comparisons with CRRES data which show that the shape of AE8 spectrum in the outer belt is too low > 5 MeV [40]. Thus, this uncertainty in the shape of the AE8 spectrum means that the data/model comparisons made here in terms of dose for specific shielding thicknesses can vary with the shielding thickness selected for the comparison.

4.3 Conclusions

Tables 1 and 2 summarize the AE8 trapped electron model comparisons with flight data for low and high altitudes, respectively, and nominal geomagnetic activity conditions. The Table 1 results are summarized from the APEX data comparisons given in Figs. 11 and 12, and Table 2 results are summarized from Figs. 15 and 16. These results indicate that the AE8 model: (a) is most accurate for low altitudes (300 – 2000 km) and inclinations above 40°, (b) overpredicts by a factor of 3 in the inner belt, and (c) can overpredict by a factor of 10 or more in other regions. AE8 is most inaccurate at the outer edge of the outer belt, corresponding to the region of geosynchronous altitude.

For times when the electron intensity is enhanced due to geomagnetic storms, at low altitudes the APEX data show that the electron dose can increase by a factor of 1.5 to about 5 for altitudes below about 750 km and inclinations above about 40° where orbits are exposed to the polar 'horns' – i.e., where the outer belt electrons reach low altitudes at polar latitudes – as shown earlier in Fig. 13. Since the inner part of the inner belt is relatively stable during geomagnetic storms, orbits in the 750 – 2000 km altitude range are relatively insensitive to electron variations with magnetic activity level.

For high altitudes, electron flux enhancements during geomagnetic storms can be very large based on the CRRES satellite measurements after the extremely large geomagnetic disturbance and particle injection event of March 1991 (Fig. 17). However,

Table 1. Measured-to-predicted electron dose ratio at low altitudes based on APEX satellite data and AE8MIN trapped electron model.

Inclination (deg)	Altitude km)	Exposure Region	Measured/AE8MIN Model
< 40	< 750	"under belts" (low flux)	2-10 (or more), highly variable
< 40	750 - 2000	inner belt, inner edge	2 - 10
> 40	300 - 750	polar horns (outer belt)	0.5 - 1.5
> 40	750 - 2000	inner belt, inner edge	1 - 2

Table 2. Measured-to-predicted electron dose ratio at high altitudes based on CRRES satellite data and AE8MAX trapped electron model for low geomagnetic activity (28.5 deg. inclination, solar maximum).

Altitude km)	Exposure Region	Measured/AE8MAX Model
2,000 - 5,000	inner belt	1/3
5,000 - 10,000	slot	1/3 - 1/50
10,000 - 30,000	outer belt, central	1/5 - 1/10
30,000 - 40,000	outer belt, outer edge	1/10 -1/100

the AE8 model overprediction for quiet times is so large that the model still overpredicts for most altitudes during high geomagnetic activity conditions. This is illustrated in Fig. 20, where we have added a curve comparing AE8MAX to CRRES data during high activity conditions after the March 1991 event to the low-activity ratio shown previously (Fig. 16).

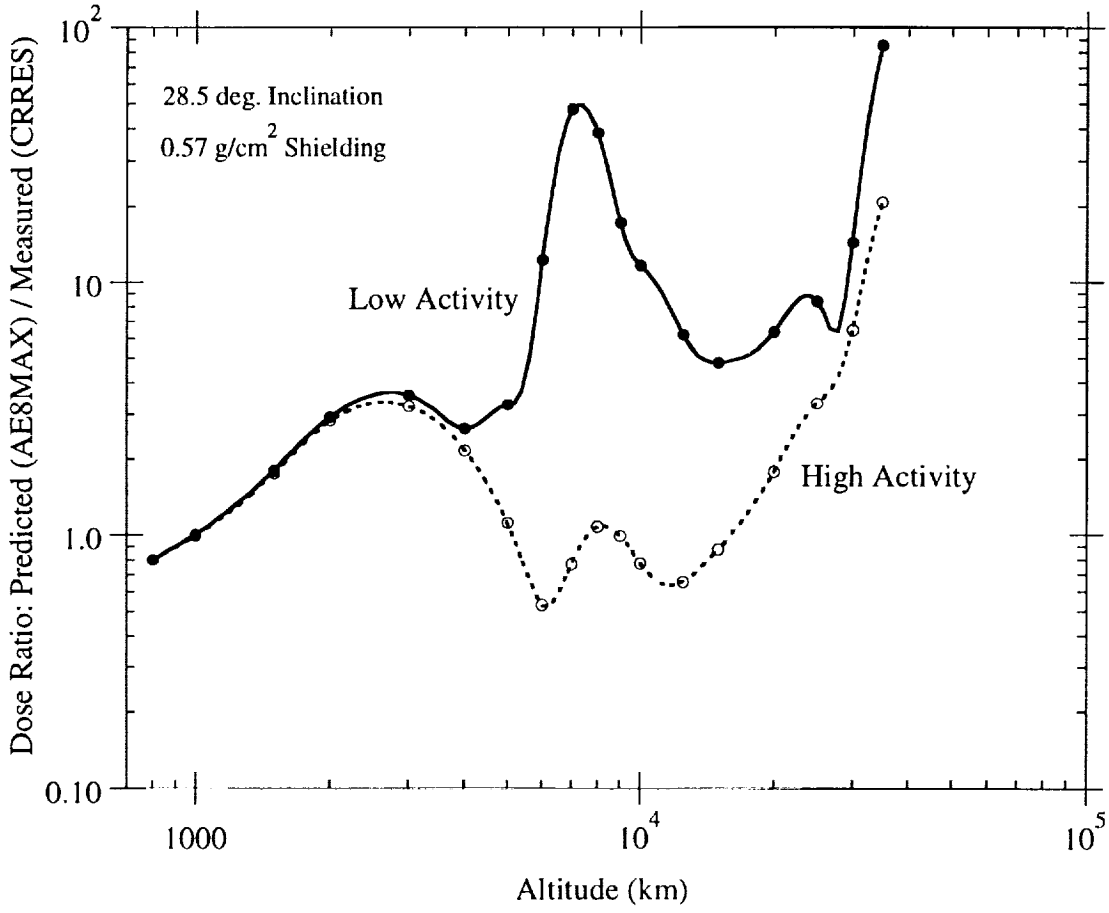

Fig. 20. Ratio of predicted electron dose using AE8MAX trapped electron flux model to dose measured on CRRES satellite for low and high geomagnetic activity conditions.

5. References

[1] Donald W. Sawyer and James I. Vette, "AP-8 Trapped Proton Environment for Solar Maximum and Solar Minimum", National Space Science Data Center, NASA Goddard Space Flight Center, NSSDC/WDC-A-R&S 76-06, 1976.

[2] M. J. Teague and J. I. Vette, "A Model of the Trapped Electron Population for Solar Minimum", National Space Science Data Center, NASA Goddard Space Flight Center, NSSDC 03-74, 1974.

[3] James I. Vette, "The AE-8 Trapped Electron Model Environment", National Space Science Data Center, Goddard Space Flight Center, NSSDC/WDC-A-R&S 91-24, Nov. 1991.

[4] T. W. Armstrong and B. L. Colborn, "Trapped Radiation Model Uncertainties: Model-Data and Model-Model Comparisons", Science Applications International Corporation, Contractor Report for NASA/MSFC, SAIC-TN-99030, September 1999.

[5] E. R. Benton and E. V. Benton, "A Survey of Radiation Measurements Made Aboard Russian Spacecraft in Low-Earth Orbit", NASA/CR-1999-020956, March 1999.

[6] T. W. Armstrong and B. L. Colborn, "TRAP/SEE Code Users Manual for Predicting Trapped Radiation Environments", Science Applications International Corporation, Contractor Report for NASA/MSFC, SAIC-TN-99010, August 1999.

[7] M. S. Gussenhoven and E. G. Mullen, "Space Radiation Effects Program: An Overview", IEEE Trans, Nucl. Sci. 40 (2), 221 (1993).

[8] M. S. Gussenhoven, E. G. Mullen, and D. H. Brautigam, "Improved Understanding of the Earth's Radiation Belts from the CRRES Satellite:, IEEE Trans. Nucl. Sci. 43 (2), 353 (1996).

[9] M. S. Gussenhoven, E. G. Mullen, D. H. Brautigam, E. Holman, C. Jordan, F. Hanser, and Dichter, "Preliminary Comparison of Dose Measurements on CRRES to NASA Model Predictions", IEEE Trans. Nucl. Sci. 38 (6), 1655 (1994).

[10] K. J. Kerns and M. S. Gussenhoven, "CRRESRAD Documentation", Phillips Laboratory, Geophysics Directorate, Hanscom AFB, PL-TR-92-2202, August 1992.

[11] M. S. Gussenhoven, E. G. Mullen, M. D. Violet, C. Hein, J. Bass, and D. Madden, "CRRES High Energy Proton Flux Maps", IEEE Trans. Nucl. Sci. 40 (6), 1450 (1993).

[12] Jeralyn D. Meffert and M. S. Gussenhoven, "CRRESPRO Documentation", Phillips Laboratory, Geophysics Directorate, Hanscom AFB, PL-TR-94-2218, July 1994.

[13] Donald H. Brautigam and Jabin T. Bell, "CRRESELE Documentation", Phillips Laboratory, Geophysics Directorate, Hanscom AFB, PL-TR-95-2128, July 1995.

[14] A. L. Vampola, "ESA Update of AE-8 Using CRRES Data and a Neutral Network", in: Radiation Belts: Models and Standards (J. F. Lemaire, D. Heynderickx, and D. N. Baker, Eds.), Geophysical Monograph 97, American Geophysical Union (1996).

[15] A. L. Vampola, "Radiation Belt Model for the PC: RADMODLS", in: Radiation Belts: Models and Standards (J. F. Lemaire, D. Heynderickx, and D. N. Baker, Eds.), Geophysical Monograph 97, American Geophysical Union (1996).

[16] M. S. Gussenhoven, E. G. Mullen, J. T. Bell, D. Madden, and E. Holman, "APEXRAD: Low Altitude Orbit Dose as a Function of Inclination, Magnetic Activity, and Solar Cycle", IEEE Trans. Nucl. Sci. 44 (6), 2161 (1997).

[17] J. T. Bell and M. S. Gussenhoven, "APEXRAD Documentation", Phillips Laboratory, Geophysics Directorate, Hanscom AFB, PL-TR-97-2117, September 1997.

[18] M. S. Gussenhoven, E. G. Mullen, R. C. Filz, D. H. Brantigam, and F. A. Hanser, "New Low-Altitude Dose Measurements", IEEE Trans. Nucl. Sci. NS-34 (3), 676 (1987).

[19] S. L. Huston and K. A. Pfitzer, "A New Model for the Low Altitude Trapped Proton Environment", IEEE Trans. Nucl. Sci. 45 (6), 2972 (1998).

[20] S. L. Huston and K. A. Pfitzer, "Space Environment Effects: Low-Altitude Trapped Radiation Model", NASA/CR-1998-208593, August 1998.

[21] M. O. Burrell and J. J. Wright, "Orbital Calculations and Trapped Radiation Mapping", NASA Marshall Space Flight Center, NASA TM X-53406, March 1966.

[22] E. V. Benton, et al., "Ionizing Radiation Exposure of LDEF (Pre-recovery Estimates)", Nucl. Tracks Radiat. Meas. 20 (1), 75 (1992).

[23] T. W. Armstrong, B. L. Colborn, and E. V. Benton, "Model Calculations of the Radiation Dose and LET Spectra on LDEF and Comparisons with Flight Date", Radiat. Meas. 26 (6), 751 (1996).

[24] T. W. Armstrong, B. L. Colborn, B. A. Harmon, and C. E. Laird, "Predictions of the Nuclear Activation of Materials on LDEF Produced by the Space Radiation Environment and Comparison with Flight Measurements", Radiat. Meas. 26(6), 765 (1996).

[25] IAGA Commission 2 Working Group 4, "Analysis of the Geomagnetic Field, International Geomagnetic Reference Field 1965.0", J. Geophys. Res. 74, 4407 (1969).

[26] Louis Hurwitz, "Mathematical Model of the 1970 Geomagnetic Field", ESSA Coast and Geodetic Survey, preprint, 4 May 1970.

[27] E. G. Stassinopoulos and G. D. Mead, "ALLMAG, GDALMG, LINTRA: Computer Programs for Geomagnetic Field and Field-line Calculations", National Space Science Data Center, NASA Goddard Space Flight Center, NSSDC 72-12, 1972.

[28] Stephen M. Seltzer, "Updated Calculations for Routine Space Shielding Radiation Dose Estimates: SHIELDOSE-2", National Institute of Standards and Technology, NISTIR-5477, Dec. 1994.

[29] G. D. Badhwar and D. E. Robbins, "Decay Rate of the Second Radiation Belt", Adv. Space Res. 17 (2), 151 (1996).

[30] G. D. Badhwar, et al., "Intercomparison of Measurements on STS-63", Radiat. Meas. 26(6), 901 (1997).

[31] G. D. Badhwar, et al., "In-flight Radiation Measurements on STS-60", Radiat. Meas. 26(1), 17 (1996).

[32] William Atwell, "The Space Radiation Environment: An Overview for Mir and ISS Missions", Proc. 34th Aerospace Sciences Meeting, American Inst. Aeronautics and Astronautics, 15-18 Jan. 1996, Reno, NV, AIAA 96-0928 (1996).

[33] G. D. Badhwar, V. A. Schurshkov, and V. A. Testlin, "Solar Modulation of Dose Rate Onboard the Mir Station", IEEE Trans. Nucl. Sci. 44(6), 2529 (1997).

[34] J. W. Watts, T. A. Parnell, and H. H. Heckman, "Approximate Angular Distribution and Spectra for Geomagnetically Trapped Protons in Low-Earth Orbit", in Proc. on High-Energy Radiation in Background Space, A. C. Rester, Jr., and J. I. Trombka (Eds.), Santibel Island, FL 1987, AIP Conf. Proc. 186, 1989.

[35] M. Kruglanski, "Engineering Tool for Trapped Proton Flux Anisotropy Evaluation", Radiat. Meas. 26(6), 953 (1996).

[36] A. L. Vampola, "Low Energy Inner Zone Protons – Revisited", in: Workshop on the Earth's Trapped Particle Environment (Geoffrey D. Reeves, Ed.), American Institute of Physics Conf. Proc. 383, AIP Press, Woodbury, N. Y. (1996).

[37] D. Heynderickx, "Comparison Between Methods to Compensate for the Secular Motion of the South Atlantic Anomaly", Radiat. Meas. 26(3), 369 (1996).

[38] K. P. Ray, et al. "Solar Cell Degradation Observed by the Advanced Photovoltaic and Electronics Experiments (APEX) Satellite", IEEE Trans. Nucl. Sci. (TBD)(1997).

[39] Bob Abel, Richard M. Thorne, and Alfred L. Vampola, "Solar Cyclic Behavior of Trapped Energetic Electrons in Earth's Inner Radiation Belt", J. Geophys. Res. 99 (A10), p. 19, 427 (1994).

[40] M. S. Gussenhoven, E. G. Mullen, and D. H. Brautigam, "Near-Earth Radiation Model Deficiencies as Seen on CRRES", Adv. Space Res. 14 (10), 927 (1994).

[41] A. L. Vampola, "The ESA Outer Zone Electron Model Update", in Proc. Environment Modelling for Space-based Applications, ESTEC, Noordwijk, NL 18-20 Sept. 1996, European Space Agency Report ESA SP-392, Dec. 1996.

[42] J. B. Blake and J. E. Cox, "The Radiation Dose in a Molniya-type Orbit", in Proc. High-Energy Radiation Background in Space (A. C. Rester and J. I. Trombka, Eds.), Santibel Island, FL 1987, AIP Conf. Proc. 186, 1989.

[43] James A. Van Allen, "Pertubations of the Earth's Inner Radiation Belt by Two Geomagnetic Storms", J. Geophys. Res. 104(A9), 20,001(1999).

[44] C. E. McIlwain, "The Radiation Belts, Natural and Artificial", Science 142, 355 (1963).

[45] M. S. Gussenhoven, E. G. Mullen, and E. Holman, "Radiation Belt Dynamics During Solar Minimum", IEEE Trans. Nucl. Sci. 36 (6), 2008 (1989).

REPORT DOCUMENTATION PAGE

Form Approved
OMB No. 0704-0188

1. AGENCY USE ONLY *(Leave Blank)*	2. REPORT DATE	3. REPORT TYPE AND DATES COVERED
	March 2000	Contractor Report (Final)

4. TITLE AND SUBTITLE
Evaluation of Trapped Radiation Model Uncertainties for Spacecraft Design

5. FUNDING NUMBERS
NAS8–40294

6. AUTHORS
T.W. Armstrong and B.L. Colborn

7. PERFORMING ORGANIZATION NAMES(S) AND ADDRESS(ES)
Science Applications International Corporation (SAIC)
1706 Prospect-Elkton Road
Prospect, TN 38477

8. PERFORMING ORGANIZATION REPORT NUMBER
M–970

9. SPONSORING/MONITORING AGENCY NAME(S) AND ADDRESS(ES)
George C. Marshall Space Flight Center
Marshall Space Flight Center, AL 35812

10. SPONSORING/MONITORING AGENCY REPORT NUMBER
NASA/CR—2000–210072

11. SUPPLEMENTARY NOTES
Prepared for NASA's Space Environments and Effects (SEE) Program
Technical Monitor: J.W. Watts

12a. DISTRIBUTION/AVAILABILITY STATEMENT
Unclassified-Unlimited
Subject Category 93
Standard Distribution

12b. DISTRIBUTION CODE

13. ABSTRACT *(Maximum 200 words)*

The standard AP8 and AE8 models for predicting trapped proton and electron environments have been compared with several sets of flight data to evaluate model uncertainties. Model comparisons are made with flux, dose, and activation measurements made on various U.S. low-Earth orbit satellites (APEX, CRRES, DMSP, LDEF, NOAA) and Space Shuttle flights, on Russian satellites (Photon–8, Cosmos–1887, Cosmos–2044), and on the Russian *Mir* Space Station. This report gives a summary of the model-data comparisons—detailed results are given in a companion report. Results from the model comparisons with flight data show, for example, the AP8 model underpredicts the trapped proton flux at low altitudes by a factor of about two (independent of proton energy and solar cycle conditions), and that the AE8 model overpredicts the flux in the outer electron belt by an order of magnitude or more.

14. SUBJECT TERMS	15. NUMBER OF PAGES
trapped radiation model uncertainties, AP8, AE8, space radiation, space ionizing radiation environments	52
	16. PRICE CODE A04

17. SECURITY CLASSIFICATION OF REPORT	18. SECURITY CLASSIFICATION OF THIS PAGE	19. SECURITY CLASSIFICATION OF ABSTRACT	20. LIMITATION OF ABSTRACT
Unclassified	Unclassified	Unclassified	Unlimited